

# Petrographic and mineralogical characterisation of fractionated pegmatites culminating in the Nb-Ta-Sn pegmatites of the Gatumba area (western Rwanda)

Niels HULSBOSCH<sup>1</sup>, Jan HERTOGEN<sup>1</sup>, Stijn DEWAELE<sup>2</sup>, Luc ANDRE<sup>2</sup> & Philippe MUCHEZ<sup>1</sup>

<sup>1</sup>*Geodynamics and Geofluids Research Group, Department of Earth and Environmental Sciences, KU Leuven, Celestijnenlaan 200E, B-3001 Leuven, Belgium*

<sup>2</sup>*Department of Geology and Mineralogy, Royal Museum for Central Africa (RMCA), Leuvensesteenweg 13, B-3080 Tervuren, Belgium*

**ABSTRACT.** The Karagwe-Ankole belt in Central Africa hosts numerous rare-metal pegmatites and Sn–W mineralised quartz veins, which are related to the granite generation that formed at  $986 \pm 10$  Ma, i.e. the G4-granites in Rwanda. This early Neoproterozoic granite generation features in the Gatumba area (western Rwanda) a linkage with a zoned cluster of barren and Nb-Ta-Sn mineralised pegmatites. The most distal pegmatite bodies in this area suffered from intense alkali metasomatism, i.e. widespread growth of albite and white mica. A petrographic and geochemical study has been carried out on the pegmatite bodies in order to determine the petrogenetic evolution of the pegmatite zonation. The compositional variation of schorl and elbaite, sampled along the regional zonation sequence, implies that the zonation can be expressed by 4 zones: a biotite, a two-mica, a muscovite and a mineralised pegmatite zone. Alkali element variations and enrichments in muscovite and K-feldspar along the zonation sequence indicate that the origin and the formation of the different pegmatite zones can be explained by a single path of fractional crystallisation. This substantial chemical differentiation accompanies in the Gatumba pegmatite field the evolution from the G4-granite generation to common pegmatites and eventually rare-element pegmatites.

**KEYWORDS:** Karagwe–Ankole belt, G4-granites, regional pegmatite zonation, LCT-family, mineral geochemistry, fractional crystallisation, alkali metals

## 1. Introduction

The Gatumba area in Rwanda is located in the Central African Mesoproterozoic Karagwe-Ankole belt (KAB) (Fig. 1A). The KAB is present in Rwanda, Burundi, the Kivu and Maniema Provinces in the Democratic Republic of Congo (DRC) and part of Uganda and Tanzania (Tack et al., 2010). The KAB forms the northern segment of the classical “Kibara belt” (Cahen et al., 1984), which was formerly thought as a single continuous orogenic belt trending northeast from the Katanga region in the Democratic Republic of Congo up to the Ankole region in southwest Uganda. Recent work (Tack et al., 2010 and references

therein) demonstrated that this traditionally defined “Kibara belt” is interrupted by the northwest-trending extension of the Ubende belt of southwest Tanzania, which has been identified as Palaeoproterozoic “Rusizian” basement (e.g. Cahen & Snelling, 1966). Consequently, Tack et al. (2010) have restricted the Kibara belt (KIB) to that part of the traditional “Kibara belt” lying southwest of the Ubende belt (i.e. the Katanga region of the DRC). The part to the northeast of the Ubende extension is now named the Karagwe–Ankole belt (KAB).

The KIB and KAB host a large metallogenic province that contains numerous granite-related ore deposits (Pohl, 1994) temporally and spatially associated with the  $986 \pm 10$  Ma S-type

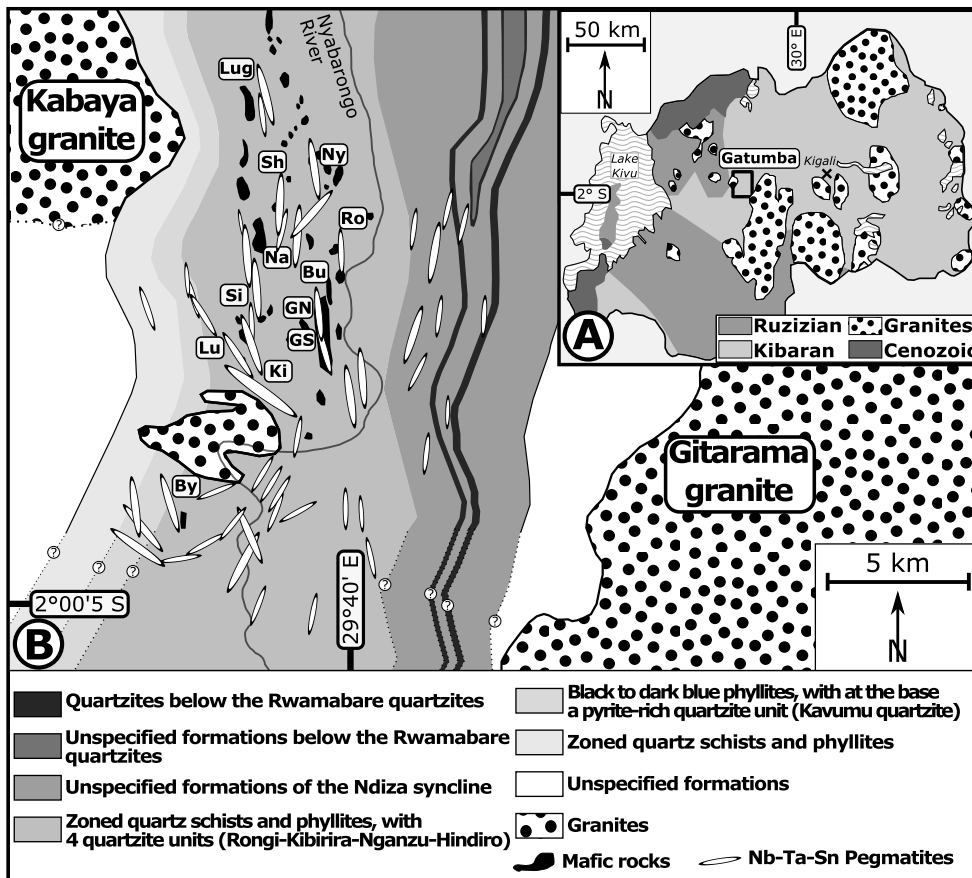


**Figure 1:** (A) Simplified geological map of Rwanda (after RMCA maps of Rwanda and Dewaele et al., 2011). The Gatumba pegmatite field is situated about 50 km west of Kigali and is indicated with a rectangle. (B) Simplified geological map of the Gatumba area, indicated with rectangle in Fig. 1A, located between the Gitarama and Kabaya plutons (adapted from Gérard (1965), Dewaele et al. (2011), Pohl (2011)). The most important outcrops of Nb-Ta-Sn mineralised pegmatite bodies are also indicated (former Nb-Ta-Sn quarries and mining concession): Bijyoyo (By), Buranga (Bu), Gatumba North (GN) and South (GS), Kirengo (Ki), Lugaragata (Lug), Luhanga (Lu), Nyarigamba (Na), Nyamissa (Ny) Rongi (Ro), Shori (Sh) and Sitwe (Si).

G4-granites (U–Pb on zircon; Tack et al., 2010), displaying two main styles of (primary) mineralisation: Sn–Nb–Ta–Li–Be pegmatite-type and Sn–W hydrothermal quartz vein-type deposits.

Recent investigations on the metallogenesis of the KAB have focussed on the timing of the columbite-tantalite and cassiterite mineralisation in highly-evolved pegmatites (e.g. Günther, 1990; Pohl, 1994; Pohl & Günther, 1991; Lehmann et al., 2008; Dewaele et al., 2008, 2011). State-of-the-art U–Pb dates (Dewaele et al., 2011) obtained on columbite-tantalite samples from rare-metal pegmatites in Rwanda (Gatumba area) overlap with the emplacement age of the G4-granites ( $986 \pm 10$  Ma; Tack et al., 2010), as well as the emplacement age of the pegmatites ( $969 \pm 8$  Ma, Rb–Sr on muscovite and whole-rock; Brinckmann & Lehmann, 1983). Younger obtained ages ( $951 \pm 15$  Ma to  $936 \pm 14$  Ma, U–Pb on columbite-tantalite; Dewaele et al., 2011) are apparently related to variable degrees of resetting by (metasomatic) post-crystallisation processes.

Several other metallogenetic studies investigated the origin and evolution of the quartz vein-type, cassiterite and wolframite-ferberite mineralisation (e.g. De Clercq et al., 2008; De Clercq, 2012; Dewaele et al., 2007b, 2010). Based on similarities in structural setting, paragenesis, host rock alteration, relative timing, and fluid and stable isotope composition, De Clercq (2012) concluded that both the Sn and W quartz vein-type deposits in Rwanda are related to the same mineralising event. Given that there is an overlap in ages between the G4-granites ( $986 \pm 10$  Ma; Tack et al., 2010) and the W-mineralised quartz veins ( $992.4 \pm 1.5$  Ma and  $984.6 \pm 2.4$  Ma,  $^{40}\text{Ar}/^{39}\text{Ar}$  on muscovite; De Clercq, 2012), and the typical association of Sn- and W-deposits with granite intrusions worldwide, De Clercq (2012) concluded that both the Sn- and W-mineralising fluids at least partly originated from the geochemically specialised G4-granites. Strong interactions of the mineralising fluid with metamorphic rocks (muscovitisation, tourmalinisation and interaction with  $\text{NH}_4^+$ -micas, feldspars and mature organic material) have subsequently overprinted the original mineralising fluid (De Clercq, 2012).

In contrast, a state-of-the-art (cf. Černý, 1991; London, 2005a, 2008) assessment of the origin and evolution of the pegmatite systems in the KAB is lacking. In addition, only few studies focus on the behaviour of trace elements during the regional pegmatitic evolution, i.e. with regards to their distribution between coexisting silicates (see Černý et al., 1985 for an overview) in the Central African pegmatite fields (Dewaele et al., 2011). The aim of this study is to evaluate the geochemical evolution of the KAB pegmatite field in the Gatumba area in the light of the current pegmatite formation and regional zonation models. These models assume that pegmatites are crystallisation products of residual melts, which separated during solidification of a granitic magma (Fersmann, 1931; London, 2005a). London (2008) defines granitic pegmatites as remarkable rocks by their diversity of rare, and in many cases, exotic minerals and the extreme enrichment in many rare elements such as Li, Be, B, F, P, Rb, Cs, REE, Nb, Ta, Zr, Hf, U and Th. They are characterised by an arranged sequence of mineral associations, a remarkable size of the individual crystals, a simultaneous crystallisation of different mineral phases and by an enrichment of highly volatile constituents. Pegmatites at Ghost Lake (Canada), for example, show a regional zonation pattern with respect to the parental granite, with the largest enrichment in incompatible elements in the more distal pegmatites (Breaks & Moore, 1992). Nevertheless, a large number of pegmatite fields (e.g. Brazil Lake, Canada; Kontak, 2006) have only an inferred, buried plutonic parent. But also in this case, the structurally highest pegmatites are particularly promising for rare-element enrichment (Kontak, 2006).

## 2. Geological setting of the Gatumba area

### 2.1. General setting

Multiple, large-scale sedimentation periods are recorded in the two independent, Mesoproterozoic sedimentary sub-basins that ultimately made up the structure of the current KAB (i.e. Eastern and Western Domains). Both sub-basins are characterised by different lithostratigraphic units and contrasting basements, with

the Western Domain overlying Palaeoproterozoic and the Eastern Domain overlying Archaean basement (Fernandez-Alonso et al., 2012). The Gatumba area forms part of the Western Domain and sedimentation in this domain started at  $\sim 1420$  Ma with the deposition of pelites belonging to the Gikoro and Pindura Groups of the Akanyaru Supergroup (sedimentation between 1420 Ma and 1375 Ma, U–Pb on zircon; Fernandez-Alonso et al., 2012). A subsequent sedimentation period (between 1222 Ma and 986 Ma, U–Pb on zircon; Fernandez-Alonso et al., 2012) in the Western Domain of the KAB is reflected in the deposition of the Cyohoha and Rugezi Groups of the Akanyaru Supergroup (see Fernandez-Alonso et al., 2012 for a detailed review of the KAB basin evolution).

The Meso- and Neoproterozoic magmatic-kinematic activity in the KAB can be divided in three main events. The metasedimentary rocks of the KAB have been affected initially by a major intracratonic bimodal magmatic event at  $\sim 1375$  Ma, also known as the “Kibaran event” (U–Pb on zircons; Tack et al., 2010). This event consisted of widespread voluminous S-type granitoid rocks, with associated subordinate mafic intrusives (Fernandez-Alonso et al., 1986; Tack et al., 2010). This granite generation (called G1-3 in Rwanda) is not associated with mineralisation (Dewaele et al., 2009). Subsequently at  $\sim 1.0$  Ga, reactivation of the underlying basement as a consequence of the far-field effect of the Southern Irumide Orogen could have been responsible for folding and thrusting of the rocks in the KAB (Tack et al., 2010), resulting in upright folds and the formation of a S2 cleavage in the Gatumba area (Dewaele et al., 2011; Fernandez-Alonso et al., 2012). Eventually at  $986 \pm 10$  Ma (Tack et al., 2010), the emplacement of a second generation of S-type granites (called G4-granites in Rwanda) was associated with a post-compression relaxation (Fernandez-Alonso et al., 2012). This barren granite generation has been described as subalkaline and strongly peraluminous, equigranular, unfoliated leucogranites with muscovite and minor biotite (Gérards & Ledent, 1970; Pohl, 1994).

Associated with the G4-granites, pegmatites intruded the KAB metasediments at  $969 \pm 8$  Ma (Brinckmann & Lehmann, 1983). The columbite-tantalite mineralisation within the pegmatites has been dated at  $975 \pm 8$  Ma and  $966 \pm 9$  Ma (U–Pb on columbite-tantalite in the Gatumba area; Dewaele et al., 2011), which overlaps with the timing of the pegmatite and the G4-granite emplacements. The G4-granite and pegmatite systems are crosscut by quartz veins (Varlamoff, 1956). The exact paragenetic position of these Sn–W mineralised quartz veins remains, however, vague (De Clercq et al., 2008; Dewaele et al., 2008, 2011; De Clercq, 2012). One cassiterite mineralised quartz vein in Burundi has been dated at  $951 \pm 18$  Ma (Rb–Sr on muscovite; Brinckmann et al., 1994). Tungsten vein ages of  $992.4 \pm 1.5$  Ma and  $984.6 \pm 2.4$  Ma obtained by De Clercq (2012) are within error identical to the ages obtained for the G4-granites, but are slightly older than the ages obtained for the Nb–Ta–Sn mineralised pegmatites by Dewaele et al. (2011).

### 2.2. Geology of the Gatumba area

The Gatumba area is situated in the western part of Rwanda, about 50 km west of Kigali (Fig. 1A) and can be considered as a representative district for the study of pegmatite mineralisation in the KAB (Dewaele et al., 2007a). The area ( $\pm 150$  km<sup>2</sup>) is located between two granitic batholiths: the Gitarama pluton to the east and the Kabaya pluton to the west (Fig. 1B), along with smaller satellite intrusions (e.g. the granite outcrop near Bijoyoyo; Fig. 1B). The metasediments of the study area consist of an alternation of Mesoproterozoic metapelites and quartzites with rare lenticular carbonates (Gérards, 1965), which all belong to the Western Domain of the KAB. Lithostratigraphically, the Mesoproterozoic rocks of the Gatumba area belong to the Akanyaru Supergroup (Fernandez-Alonso et al., 2012). The geological map (sheet Ruhengeri, scale 1/100,000; Royal Museum for Central Africa, 1991) combined with the lithostratigraphic map of the Gatumba area (scale 1/250,000; Royal Museum for Central Africa, 1981) indicates the presence of the Gikoro, Pindura and Cyohoha Groups, between the granite massifs of Gitarama and Kabaya. The Gatumba area is structurally situated on the western limb of the Ndiza syncline. The core of the syncline is located about 20

km to the east of the Gatumba area sensu stricto and hosts the Rwamabare quartzites (Gérards, 1965).

The metasedimentary rocks in the Gatumba area are intruded by dolerites and pegmatite bodies. The dolerite emplacement is thought to have been pre-kinematic, since they are crosscut by the S2 cleavage and folded together with the metasediments (Gérards, 1965). The mafic rocks are locally crosscut by the pegmatitic bodies, which are emplaced along these S2 cleavage planes in the phyllitic rocks. Consequently, the pegmatite emplacement is considered as syn- to post-kinematic (Gérards, 1965; Dewaele et al., 2011; Fernandez-Alonso et al., 2012).

The regional metamorphic grade of the area has been reported as lower greenschist facies (Baudet et al., 1988). The metapelitic rocks in the Gatumba area range from sericite-rich phyllites to muscovite- or sometimes biotite-rich mica schists. Thermal overprinting of the regional lower greenschist rocks, induced by granite emplacement, has been described by Gérards (1965). Typical minerals indicative for a thermal metamorphism in the rocks of the Gatumba area are biotite, poikiloblastic chlorite, garnet, andalusite and very locally sillimanite. Rare dolomite lenses, when affected by thermal metamorphism, contain mineral assemblages of tremolite, chlorite, zoisite and titanite, in addition to newly formed quartz (Gérards, 1965).

**2.3. Geology and typology of the pegmatites**

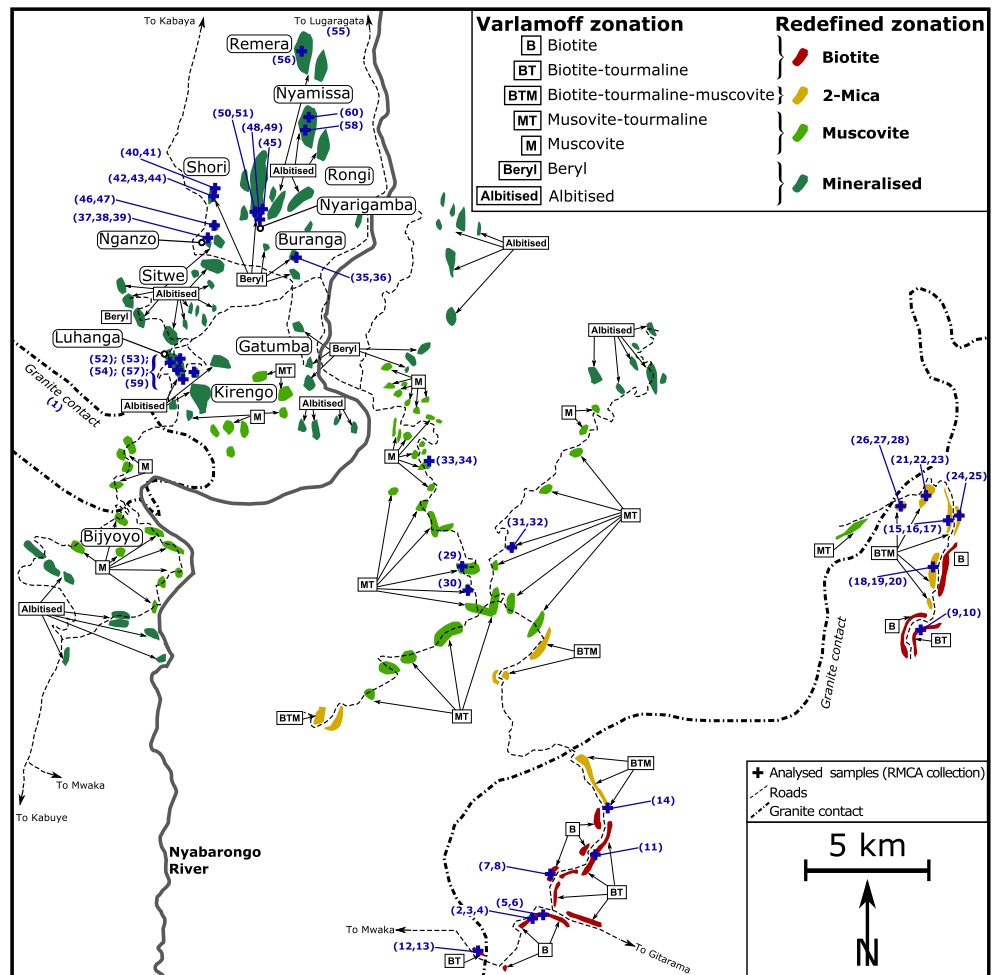
The Gatumba area is characterised by the presence of numerous rare-metal pegmatites, which are variably mineralised in columbite-tantalite and/or cassiterite. Beryl, spodumene, tourmaline, apatite, amblygonite and rare phosphates are the most important accessory minerals (Varlamoff, 1954a, 1954b). The dimension of the individual pegmatite bodies is rather variable. The thickness can vary between several centimetres to 30 m and the length ranges from tens of meters up to 2400 m. More than 130 large pegmatite bodies have been identified and mapped by the former colonial mining companies Minétain and Somirwa (Dewaele et al., 2011 and references therein). The pegmatite field

has seen some historical, semi-industrial production, mainly from highly weathered pegmatite outcrops or from secondary (alluvial or eluvial) deposits. Between 1929 and 1985, production reached ~17,600 metric tons of mixed cassiterite and columbite-tantalite concentrate (unpublished data Somirwa). Today, there is mainly an artisanal production. The reserves have been estimated at ~950 metric tons, with further resources between 2400 and 3400 metric tons of cassiterite (unpublished data Somirwa). The economic potential of the hard-rock pegmatites has never been evaluated. The Gatumba area is currently under prospecting rights of Gatumba Mining Concession (GMC).

In the Gatumba area, pegmatite emplacement as well as primary Nb-Ta mineralisation overlap with the general timing of the G4-granite emplacements in the KAB (see 2.1.). Varlamoff (1954a) suggested that the Gitarama pluton was the parental intrusion for the pegmatites in the Gatumba area, based on their mutual spatial relation (Fig. 1B). However no decisive radiometric or geochemical arguments are available in literature to support the G4-affinity of the Gitarama granite. Pohl (1994) reported, moreover, that an important feature of the “Kibara granites” (i.e. G1-3 and G4 granites in Rwanda) is their frequent occurrence in well-defined composite plutons. As such, the inferred parental granitic source for the Gatumba pegmatite field still remains unknown. A composite (G1-3 to G4) origin for the Gitarama pluton or even an unidentified, buried plutonic G4-intrusion are legitimate alternatives for the concept of a primary G4-origin of the Gitarama pluton.

A regional mineralogical zonation within the Gatumba pegmatite field has been documented by Varlamoff (1954a, 1954b, 1961, 1963, 1972). It comprises nine distinct mineralogical zones which seem to occur along the northwestern margins of the Gitarama pluton and of which seven are associated with pegmatite occurrences: (1) biotite, (2) biotite-tourmaline, (3) biotite-tourmaline-muscovite, (4) muscovite-tourmaline, (5) muscovite, (6) beryl and (7) albitised pegmatites (Fig. 2). Zones (8) and (9) are exclusively for quartz veins accessorially

**Figure 2:** Map of outcropping pegmatite bodies in the Gatumba pegmatite field. The map displays the zonation pattern of the barren, common pegmatite bodies (i.e. biotite, biotite-tourmaline, biotite-tourmaline-muscovite, muscovite-tourmaline and muscovite zones) and Nb-Ta-Sn mined pegmatites (from north to south the former mining concessions of Lugaragata, Remera, Nyamissa, Shori, Rongi, Nyarigamba, Buranga, Nganzo, Sitwe, Luhanga, Gatumba [North and South], Kirengo and Bijyoyo). The mineralogical, Varlamoff zonation is according to Varlamoff (1954a, 1954b, 1961) and the 1/50,000 mining map of the Gatumba sector (unpublished map of N. Varlamoff, November 1956, RMCA collection). The colour code, which is applied to the different pegmatite zones, is according to our redefined, chemical zonation. The sample locations are indicated with blue crosses and complementary sample numbers between brackets (1 to 60). The sample numbers also correspond to the chemical analyses on the separated minerals (Tables 2 & 3). Sample 55 of the former Lugaragata mining concession is not shown on this map (located ~6 km north of the former Remera mining concession; sample 56).



mineralised in cassiterite (Varlamoff, 1954a, 1954b, 1956, 1972). Pegmatites belonging to zones 6 and 7 are both characterised by a variable degree of Nb-Ta-Sn mineralisation. These most evolved pegmatites are also affected by an intense metasomatic-hydrothermal alteration resulting in albitisation and greisenisation (Dewaele et al., 2011). All the pegmatite bodies of the Gatumba area were emplaced along the S2 cleavage and no crosscutting relation between pegmatites of different zones could be observed in the field (Fig. 2; additional observations made in the field by S. Dewaele).

The most evolved pegmatites of the area, i.e. pegmatites assigned to zones 6 and 7, are classified by Dewaele et al. (2011) as belonging to the LCT (lithium-caesium-tantalum) family according to the petrogenetic-geochemical classification of Černý & Ercit (2005). Further classification accommodates the pegmatites in the rare-element class and lithium subclass. Based on the rare-element mineralogy, the Gatumba area pegmatites include representatives of the beryl-type (beryl-columbite subtype), complex-type (spodumene subtype) and albite-spodumene type (Dewaele et al., 2011). Dewaele et al. (2008, 2011) have determined the paragenetic sequence of the mineralisation in the most evolved and hydrothermally altered pegmatites of the Gatumba area. Based on petrographic observations and stable isotope data, these authors concluded that the columbite-tantalite and cassiterite mineralisation mainly formed during two distinct stages: the columbite-tantalite and some of the cassiterite formed during an earlier stage of crystallisation of the pegmatites prior to the albitisation, while the major part of the cassiterite formed during the later metasomatic-hydrothermal overprint, associated with sericitisation and muscovitisation of local zones of the pegmatites (i.e. the so-called greisenisation; cf. Štemprok, 1987). The presences of columbite-tantalite in the pegmatites and not in the hydrothermal alteration zones can be explained by low solubility of Nb and Ta in aqueous solutions (Linnen & Cuney, 2005). Sericitisation and cassiterite precipitation occurred from fluids with a H<sub>2</sub>O-CO<sub>2</sub>-NaCl-KCl composition (Dewaele et al., 2008).

### 3. Materials and methods

A petrographic study was carried out on the seven distinct pegmatite zones as defined by Varlamoff (1954a) by using a transmitted and incident light microscope type Olympus BX60. Photomicrographs of thin sections were taken using a Deltapix DP200 image capturing system mounted on a Leica DM LM/P optical microscope. The samples were taken from the rock collection of the Royal Museum for Central Africa (RMCA). The majority of these samples were collected during historical field campaigns of Varlamoff (e.g. 1954a) and Gérards (1965). The exact position of the pegmatite samples is known from (un) published field and archive data of the RMCA (Fig. 2).

Mineral separates of feldspar, biotite, muscovite and tourmaline that represent the whole gamut of regional pegmatite zonation and alteration have been analysed for major, minor and trace elements. The geochemical data of the separates were obtained by inductively coupled plasma-optical emission spectrometry (ICP-OES), type Varian 720 ES (KU Leuven), and by inductively coupled plasma-quadrupole mass spectrometry (ICP-QMS), type Thermo Scientific X-Series 2 (RMCA). Pegmatite rocks are crushed and sieved to achieve samples with a grain size between 500 µm and 1000 µm. These grains are subsequently hand-picked and microscopically sorted with a Novax Holland stereomicroscope to obtain pure mineral separates. Each pure mineral sample (~1 g) is pulverised using a Retsch MM200 mixer mill with agate grinding tools. An adapted lithium metaborate flux procedure of Suhr & Ingamells (1966), with 0.100 g of sample and 0.500 g of Spectroflux 100A LiBO<sub>2</sub> heated in carbon crucibles at 1020°C for 12 minutes, is applied as solution technique for ICP-OES as well as for ICP-MS analysis. Standards BCR-1, BCS-269, BR, GA, GBW-7411, MRG-1, NBS 70a, NIM-G and NIST 620 are used to cover the broad compositional range of the mineral samples.

Lithium and boron are not analysed due to the use of the lithium metaborate flux procedure prior to ICP-OES and ICP-QMS analyses. Non-100% oxide sums are a direct result of this

analytical procedure (Table 2). Moreover, oxide sums are often not reported for pegmatite minerals (cf. Neiva, 1995; Alfonso et al., 2003). Especially, schorl (hydrous and B-bearing) and elbaite (hydrous and B-Li-bearing) demonstrate deviating oxide sums. Micas and feldspars from the Nb-Ta-Sn mineralised pegmatites and greisens indicate that Li (and also H<sub>2</sub>O in the case of micas, and probably B and F; Roda et al., 2007) are enriched in these minerals up to several weight percentages. Our major and trace element compositions are in accordance to compositions reported for these minerals from the Gatumba pegmatites (Lehmann et al., 2008) as well as from other LCT-pegmatites worldwide (e.g. Jolliff et al., 1987; Alfonso et al., 2003; Roda et al., 2007; London, 2008).

## 4. Petrography

### 4.1. Observations

Petrographic investigation of the pegmatites throughout the zonation sequence indicates that the mineralogical variation within a given pegmatite zone is limited in the early zones 1 to 5 of Varlamoff (1954a). The main minerals in the biotite (zone 1) and biotite-tourmaline pegmatites (zone 2) are quartz, microcline with typical tartan twinning, minor plagioclase and biotite. Microscopic textures include perthite intergrowths of albite-oligoclase (Michel-Levy method: An<sub>20</sub>; Tobi & Kroll, 1975) in microcline (Plate 1A), minor sericitisation of microcline (<1%), kinking of biotite cleavage, deformation twinning in feldspars as well as undulose extinction and sutured boundaries of both quartz and K-feldspar. Black tourmaline in the biotite-tourmaline pegmatites (zone 2) occurs as graphic intergrowths with quartz crystals and can be identified as a Fe-rich member of the complete solid solution between the Fe- and the Mg-rich end-members schorl and dravite. Biotite-tourmaline-muscovite pegmatites (zone 3) are characterised by the occurrence of centimetre-sized sheets of greyish muscovite, macroscopically intergrown with biotite (Plate 1B) and microscopically observable as spherulitic muscovite. The main mineralogy is comparable to that in zone 2 pegmatites. The abundant black tourmalines in zone 3, which equally display graphic intergrowths with quartz, also belong to the schorl-dravite series. Accessory small (< 50 µm) monazite crystals occur enclosed in or isolated between the main rock forming mineral phases such as microcline, blocky K-feldspar or muscovite (Plate 1C). Muscovite-tourmaline and muscovite pegmatites (zone 4 and 5) consist of quartz, white microcline with typical tartan twinning, minor plagioclase, grey-coloured muscovite and minor blocky pink K-feldspar. Biotite is absent in these pegmatites. Black schorl-dravite series tourmaline is a typical constituent of the muscovite-tourmaline pegmatites (zone 4). Monazite is also observed in both zones 4 and 5 and occurs enclosed by or interlocked between microcline crystals or as inclusions in rare, subhedral apatite crystals. Small (< 5mm) greenish-blue beryl crystals can be found as an accessory mineral in the muscovite pegmatites (zone 5).

The mineralised pegmatites (zones 6 and 7) contain respectively elbaite (Plate 1D) and lepidolite (Plate 1E) and both zones show the development of massive greisen bodies. A detailed description of these pegmatite zones with attention to the secondary alteration assemblages (albitisation and greisenisation), the columbite-tantalite mineralogy and the mineral paragenesis can be found in Varlamoff (1954a, 1954b, 1956, 1961, 1963), Melcher et al. (2008a, 2008b, 2009a, 2009b) and Dewaele et al. (2011). Macro- and microscopic observations on pre-alteration assemblages in the mineralised pegmatites indicate the occurrence of pink K-feldspar (mainly orthoclase and microcline), white albite-oligoclase, quartz, dark-green Li-muscovite, lepidolite, elbaite, multi-coloured beryl, apatite, spodumene, columbite-tantalite and minor cassiterite as the primary magmatic minerals. Lepidolite occurs as massive, fine-grained and non-oriented violet-gray to lavender-coloured aggregates (Plate 1E). Microscopic traces of quartz and orthoclase are also present inside the lepidolite matrix (Plate 1F). In addition, massive decimetre-sized dark-green elbaite has been observed in an assemblage with quartz (Plate 1D) and accessory platy albite (so-called cleavelandite; Fisher, 1968). Cleavelandite

Zone	Name	Main minerals	Accessory minerals
1	<i>Biotite pegmatites</i>	Microcline, plagioclase, quartz, minor biotite	Almandine-pyrope-spessartine garnet, minor black tourmaline
2	<i>Biotite-tourmaline pegmatites</i>	Microcline, biotite, black tourmaline, (plagioclase)	Almandine-pyrope-spessartine garnet, minor zircon
3	<i>Biotite-muscovite-tourmaline pegmatites</i>	Microcline, quartz, greyish muscovite, abundant black tourmaline, biotite	Monazite
4	<i>Muscovite-tourmaline pegmatites</i>	Microcline, quartz, greyish muscovite, black tourmaline,	Monazite, apatite
5	<i>Muscovite pegmatites</i>	Microcline, abundant quartz, greyish muscovite, pink K-feldspar	Monazite, black tourmaline, apatite, minor green beryl
6	<i>Beryl pegmatites</i>	Microcline, pink K-feldspar, quartz, dark green muscovite, beryl, elbaite, amblygonite, spodumene, minor albitisation and greisenisation (saccharoidal albite with cleavelandite and light-green/greyish muscovite)	Black tourmaline, apatite columbite-tantalite, cassiterite, phosphates
7	<i>Albitised pegmatites</i>	Microcline, quartz, dark green muscovite, lepidolite, pink K-feldspar, profound albitisation and greisenisation (saccharoidal albite with cleavelandite and light-green/greyish muscovite)	Abundant cassiterite, columbite-tantalite, coloured tourmaline (elbaite), beryl, spessartine, black tourmaline at the contact with metasediments

**Table 1:** Compilation of the mineralogy of the different pegmatite zones in the Gatumba area based on own observations and modifications from Varlamoff (1954b).

has formed by the albitisation of primary K-feldspars (Dewaele et al., 2011). The lack of replacement textures and cross-cutting relations between cleavelandite and elbaite indicates a primary origin for elbaite.

The majority of the pegmatite samples in zones 6 and 7 display evidence of albitisation, most often at the expense of the (alkali) feldspars, but also of primary quartz-muscovite assemblages. Secondary albite patches crosscut and replace the primary assemblages, with two habits, saccharoidal albite and platy cleavelandite. The difference in habit is visible in hand specimens and the cleavelandite lath-shaped morphology is distinctly seen under the microscope. Saccharoidal secondary albite is always anhedral, whereas the platy variety is generally sub- to euhedral. Saccharoidal grains can be up to a few millimetres in size, whereas cleavelandite is generally less than 1 mm in length.

Either barren or cassiterite-bearing greisens may be found in the incomplete metasomatic/hydrothermal altered pegmatites of zones 6 and 7. Quartz, non-oriented light-green to greyish Li-

muscovite and minor, but variable, quantities of orthoclase form their bulk composition. Other greisen-related minerals, such as topaz, tourmaline and fluorite, are absent. Quartz crystals in the matrix of the greisens are enlarged and show recrystallisation textures such as undulose extinction and bulging.

**4.2. Interpretation**

The mineral sequence found in this study is consistent with the reported mineral paragenesis of pegmatites from the Gatumba area (Varlamoff, 1954a, 1954b; Dewaele et al., 2008, 2011), but the present work allows to go into more detail concerning the accessory minerals, the “exotic” minerals lepidolite and elbaite and the classification of the greisen-type rocks. An overview of the mineralogy of the different pegmatite zones based on both literature and our own data is given in Table 1.

Although Varlamoff (1954a) observed (rare) monazite in zone 1 biotite pegmatites, he did not signal its presence in zone 3 biotite-tourmaline-muscovite pegmatites and in outmost zones

**Table 2:** Main composition of the minerals from the different pegmatite zones (ICP-OES analysis); B = Biotite, BT = Biotite-tourmaline, BTM = Biotite-tourmaline-muscovite, MT = Muscovite-tourmaline, M = Muscovite, Min = Mineralised pegmatites, Gra = granite and Gr = Greisens. Minerals: Afs = pink K-feldspar, Ab = albite, Bt = biotite, Elb = elbaite, Lpd = lepidolite, Mc = Microcline, Ms = muscovite, Olg = oligoclase, Or = orthoclase and Srl = schorl. (BDL = Below Detection Limit)

Nr.	1	2	3	4	5	6	7	8	9	10	11	12	13	14	15	16	17	18	19	20
Zone	Gra	B	B	B	B	B	B	B	B	B	B	B	B	B	B	B	B	B	B	B
Mineral	Bt	Bt	Or	Mc	Or	Bt	Ab	Bt	Olg	Bt	Srl	Or	Srl	Ms	Bt	Ms	Ab	Srl	Ms	Or
SiO <sub>2</sub>	38,62	35,79	66,40	64,73	63,20	35,53	65,05	35,64	65,39	36,01	34,30	63,81	35,34	48,37	38,85	49,04	67,41	35,86	45,54	62,89
TiO <sub>2</sub>	3,01	2,22	0,01	0,01	0,01	2,26	0,01	2,31	0,01	1,51	0,37	0,01	0,46	0,19	0,40	0,04	0,00	0,32	0,14	0,01
Al <sub>2</sub> O <sub>3</sub>	16,27	18,95	18,06	18,83	18,25	18,31	20,74	19,21	20,87	20,62	31,37	18,25	31,47	33,40	22,77	32,73	19,39	34,09	35,62	18,81
FeO(t)	19,77	21,08	0,05	0,05	BDL	21,59	0,03	20,87	0,01	20,62	11,55	0,05	11,62	1,49	17,80	1,77	0,02	11,34	1,50	0,02
MnO	0,40	0,38	<0,01	<0,01	<0,01	0,40	<0,01	0,41	<0,01	0,24	0,17	<0,01	0,18	0,01	0,18	0,01	0,00	0,08	0,01	<0,01
MgO	7,62	5,77	0,03	0,04	0,02	5,83	0,03	5,51	0,02	3,43	4,06	0,02	4,31	0,47	1,65	0,33	0,02	2,70	0,38	0,02
CaO	0,75	0,04	0,24	0,44	0,08	0,06	1,89	0,08	1,86	0,06	0,25	0,01	0,26	0,06	0,05	0,03	1,18	0,16	BDL	0,01
Na <sub>2</sub> O	0,34	0,07	2,81	4,51	3,22	0,06	9,86	0,07	9,91	0,17	2,20	0,48	2,27	0,50	0,17	0,62	9,75	1,72	0,70	0,50
K <sub>2</sub> O	8,71	9,13	11,81	9,26	11,52	8,96	0,58	9,00	0,59	6,46	0,06	14,85	0,08	10,27	6,42	9,66	0,64	0,09	10,10	14,95
P <sub>2</sub> O <sub>5</sub>	0,38	0,03	0,20	0,20	0,20	0,05	0,18	0,03	0,15	0,06	0,01	0,17	0,01	0,07	0,33	0,06	0,26	0,02	0,05	0,48
Sum	95,85	93,46	99,61	98,07	96,48	93,04	98,38	93,13	98,80	89,18	84,34	97,65	86,00	94,82	88,61	94,31	98,67	86,38	94,04	97,69
Nr.	21	22	23	24	25	26	27	28	29	30	31	32	33	34	35	36	37	38	39	40
Zone	BTM	MT	MT	MT	M	M	Min	Min	Min	Min	Min	Min								
Mineral	Bt	Mc	Ms	Srl	Ms	Olg	Ms	Bt	Srl	Srl	Ms	Srl	Mc	Ms	Ab	Srl	Afs	Ms	Or	Ms
SiO <sub>2</sub>	37,80	66,20	51,23	37,79	45,63	64,30	49,23	40,36	35,67	38,48	45,90	35,37	66,55	47,75	69,57	34,20	67,60	45,00	63,64	44,72
TiO <sub>2</sub>	0,46	<0,01	0,05	0,17	0,09	0,00	0,04	0,44	0,10	0,09	0,17	0,32	0,00	0,03	0,00	0,07	<0,01	0,05	<0,01	0,04
Al <sub>2</sub> O <sub>3</sub>	21,89	19,85	31,33	31,48	34,85	20,30	31,93	20,46	33,09	31,59	35,77	33,91	18,16	34,34	17,40	32,95	17,95	35,11	18,83	36,11
FeO(t)	19,15	0,04	1,60	12,74	1,77	0,03	1,74	20,55	12,93	12,12	1,55	11,47	0,04	1,24	0,02	15,02	0,03	1,85	0,02	1,36
MnO	0,19	<0,01	0,01	0,14	0,02	<0,01	0,01	0,21	0,12	0,11	0,01	0,08	0,01	0,03	<0,01	0,42	<0,01	0,02	<0,01	0,02
MgO	1,77	0,02	0,33	1,28	0,42	0,02	0,35	1,87	1,62	1,65	0,46	2,64	0,02	0,04	0,02	0,09	0,02	0,17	0,03	0,05
CaO	0,06	0,84	<0,01	0,04	BDL	1,49	BDL	0,15	0,03	0,04	BDL	0,17	0,09	0,03	0,14	0,10	0,68	0,03	0,61	BDL
Na <sub>2</sub> O	0,32	8,07	0,44	1,60	0,54	11,67	0,48	0,33	1,73	1,61	0,60	1,71	6,28	0,72	10,39	2,09	10,50	0,78	2,82	0,67
K <sub>2</sub> O	6,53	3,93	9,35	0,09	10,14	0,94	9,39	6,40	0,15	0,11	10,38	0,10	6,27	9,67	0,11	0,10	0,40	9,94	12,01	10,01
P <sub>2</sub> O <sub>5</sub>	0,18	0,23	0,07	0,01	0,05	0,26	0,05	0,14	0,02	0,01	0,03	0,02	0,34	0,10	0,27	0,07	0,47	0,07	0,65	0,07
Sum	88,35	99,18	94,42	85,35	93,50	99,02	93,22	90,92	85,46	85,81	94,88	85,78	97,76	93,96	97,93	85,12	97,64	93,03	98,61	93,06
Nr.	41	42	43	44	45	46	47	48	49	50	51	52	53	54	55	56	57	58	59	60
Zone	Min	Gr	Gr	Gr	Gr	Gr	Gr													
Mineral	Ab	Ms	Ab	Or	Lpd	Ab	Elb	Elb	Elb	Elb	Elb	Mc	Afs	Ms						
SiO <sub>2</sub>	65,12	45,54	65,88	61,64	48,96	66,58	45,68	35,94	36,17	36,40	36,73	63,81	63,85	63,15	46,48	44,27	47,00	47,15	43,91	48,22
TiO <sub>2</sub>	0,01	0,04	0,01	0,01	0,01	0,01	0,05	0,05	0,04	0,04	0,05	0,01	0,01	<0,01	0,07	0,07	0,05	0,05	0,05	0,06
Al <sub>2</sub> O <sub>3</sub>	19,27	34,70	19,67	18,50	28,19	18,71	34,96	36,39	36,14	37,14	37,35	18,64	18,51	18,88	35,27	35,07	34,26	33,71	35,71	32,61
FeO(t)	0,10	1,46	0,04	0,03	0,03	0,04	1,62	4,76	7,01	5,01	4,52	0,04	0,02	0,01	0,83	1,67	0,71	1,48	0,96	1,47
MnO	<0,01	0,01	<0,01	<0,01	0,26	<0,01	0,01	0,61	0,47	0,64	0,65	<0,01	<0,01	<0,01	0,05	0,05	0,02	0,06	0,02	0,05
MgO	0,03	0,11	0,03	0,02	0,02	0,04	0,32	0,05	0,06	0,08	0,07	0,03	0,03	0,02	0,04	0,09	0,13	0,05	0,11	0,05
CaO	0,02	0,01	0,04	0,01	BDL	0,63	0,07	0,31	0,09	0,28	0,37	0,14	0,09	0,02	BDL	BDL	BDL	BDL	BDL	BDL
Na <sub>2</sub> O	10,90	0,80	10,91	1,28	0,26	10,85	0,83	2,34	2,70	2,44	2,36	2,41	1,99	1,11	0,86	0,58	0,52	0,68	0,64	0,65
K <sub>2</sub> O	0,30	9,37	0,25	13,28	10,09	0,18	9,89	0,40	0,07	0,27	0,40	12,21	12,94	13,80	9,50	9,77	9,49	9,63	9,71	9,23
P <sub>2</sub> O <sub>5</sub>	0,12	0,06	0,34	0,64	0,03	0,41	0,10	0,03	0,01	0,02	0,03	0,15	0,14	0,46	0,05	0,06	0,05	0,04	0,06	0,04
Sum	95,87	92,11	97,16	95,41	87,84	97,43	93,53	80,88	82,77	82,33	82,52	97,44	97,58	97,46	93,15	91,62	92,24	92,84	91,16	92,38

4 and 5. Small accessory monazite (< 50  $\mu\text{m}$ ) occurs enclosed in or isolated between the main rock-forming minerals such as microcline and muscovite of zone 3 pegmatites, indicating that it is a primary liquidus phase (Montel, 1993). Monazite also occurs in pegmatites of zones 4 and 5 as inclusions in, or interlocked between, microcline crystals or as inclusions in rare, subhedral apatite crystals, indicating that the accessory phase is stabilised due to saturation in the pegmatite melt (Montel, 1993).

According to Varlamoff's (1961) field data, lepidolite is a mineral of the pegmatite zone 7, present in albitised zones. As a consequence of our observation that trace amounts of quartz and orthoclase are relicts after albitisation and are preserved within lepidolite aggregates, lepidolite has a secondary origin in such pegmatites. Secondary replacement assemblages of lepidolite in LCT-family pegmatites are also observed in other studies (e.g. Černý et al. 1985; Beurlen et al. 2011). Such secondary Li-rich micas can occur as a pseudomorphic replacement of either aluminosilicates (feldspars, Li-aluminosilicates, tourmaline, pollucite ...) or rare phosphates by the action of late F-bearing aqueous fluids (London, 2008 and references therein). On the contrary, primary, non-replacing lepidolite has also been observed in LCT-type pegmatites (e.g. Hawthorne & Černý 1982; Novák & Černý 1998; Brown & Wise 2001) and been interpreted as a crystallisation product from a residual melt. In general, lepidolite assemblages, either primary or secondary in origin, are typically found close to the pegmatite cores which are the latest units to consolidate (e.g. Varlamoff, 1963, Černý et al., 1985; Brown & Wise, 2001). Elbaite occurs exclusively in pegmatite zone 6 (Varlamoff, 1961). The close association of elbaite with quartz could point towards a quartz core development (cf. London, 2008; Plate 1D). According to Varlamoff (1961), a quartz core only developed in zone 6 pegmatites. In contrast to highly-evolved pegmatites (London, 2008), an internal zonation is poorly developed and often not observable in the pegmatites of the Gatumba field. In pegmatites of the zones 6 and 7, the alteration of feldspar to muscovite is only partial. Therefore, the muscovite-rich rocks of the greisens family can be described as "incomplete" quartz-mica greisens according to the scheme of Štemprok (1987).

## 5. Geochemistry

### 5.1. Major elements

#### 5.1.1. Feldspars

There are no systematic variations in major elements among the feldspars from the different zones (Table 2). The orthoclase component of the K-feldspar ranges between  $\text{Or}_{69}$  and  $\text{Or}_{95}$ , with two analysed K-feldspars with respectively  $\text{Or}_{36}$  and  $\text{Or}_{51}$ . In

general, the K-feldspar from mineralised pegmatites has a high potassium content ( $>\text{Or}_{80}$ ). Feldspars belonging to the plagioclase series vary between  $\text{An}_{0.2}$  and  $\text{An}_{17}$ . Albite with a composition between  $\text{An}_{0.2}$  and  $\text{An}_{6.4}$  is exclusively found in the mineralised pegmatites (zones 6 and 7). It occurs as sub-centimetre grains with saccharoidal and cleavelandite morphologies, characterising them as secondary albite.

#### 5.1.2. Micas

Dark-green muscovites in the mineralised pegmatites and light-green/greyish muscovite in the greisens are poor in MgO, FeO(t), and  $\text{TiO}_2$  compared to the grey-coloured muscovites from the non-mineralised pegmatites. The total content of the latter elements decreases along the Varlamoff zonation (Table 2). Lepidolite is characterised by a lower  $\text{Al}_2\text{O}_3$  content and is enriched in Mn, due to the incorporation of Mn in the octahedral layer of lepidolite instead of Mg,  $\text{Fe}^{2+}$  and vacancies in white and dark micas (London, 2008).

Biotite is sampled from the first three pegmatite zones. A biotite from the Bijyoyo granite serves as reference (sample location in Fig. 2). The biotite compositions show a decreasing Mg content along the Varlamoff zonation, evolving from 4.60 wt% to 0.99 wt%, and a small decrease of the Fe content (21.59 wt%–17.80 wt% FeO(t); Table 2). The decrease of the Fe content is not entirely in accordance with the regional granite-pegmatite system since the biotite from the Bijyoyo granite (19.77 wt% FeO(t)) plots in the composition range of biotites from pegmatites of the Gatumba area. However, a normalisation by using the  $\text{Fe}_{\text{tot}} / (\text{Fe}_{\text{tot}} + \text{Mg})$  ratio in biotite (Fig. 3A–B) defines a positive trend with the Varlamoff zonation. The ratio increases from 0.78 in biotite from the granite sample to 0.93 in biotite from biotite-tourmaline-muscovite pegmatites. The Mn (Fig. 3A) and Ti (Fig. 3B) concentration in biotite decreases along the zonation.

#### 5.1.3. Tourmalines

Tourmaline from different pegmatites can petrographically be subdivided in black schorl and green elbaite variants. ICP-OES analyses confirm the petrographic interpretation that tourmalines of the biotite-tourmaline, biotite-tourmaline-muscovite and the muscovite-tourmaline pegmatites belong to the schorl-dravite solid solution series (Table 2). All these black tourmalines have compositions that plot near the schorl end-member (Fig. 4), with  $\text{Fe}_{\text{tot}} / (\text{Fe}_{\text{tot}} + \text{Mg})$  ratios changing from 0.78 in biotite-tourmaline pegmatites, 0.84 in biotite-muscovite-tourmaline to 0.92 in muscovite-tourmaline pegmatites (Fig. 3C–D). Because of the large amount of possible substitutions, tourmaline  $[\text{XY}_3\text{Z}_6(\text{BO}_3)_3\text{Si}_6\text{O}_{18}(\text{OH})_4]$  is classified in terms of the end-member substitutions for the Y-cation site (Hawthorne & Henry, 1999). The X-site is typically occupied by Na, but may also accommodate variable amounts of Ca, Mg and vacancies. The

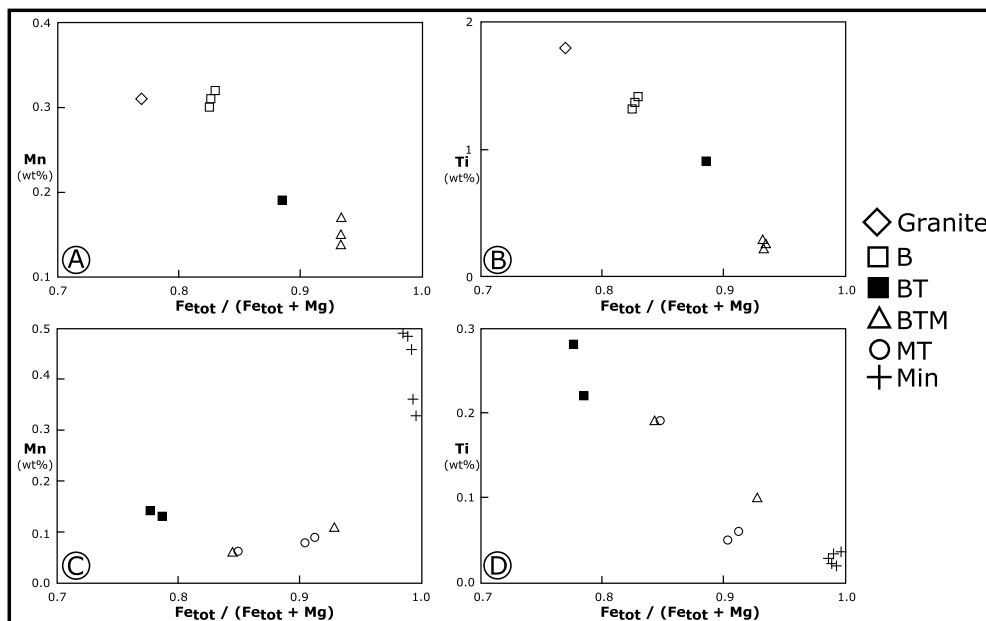


**Figure 3:** Structural components Mn (A) and Ti of biotite (B) and tourmaline (C & D) according to their evolution along the pegmatite zonation expressed by the  $\text{Fe}_{\text{tot}} / (\text{Fe}_{\text{tot}} + \text{Mg})$  ratio (G = granite, B = biotite, BT = Biotite-tourmaline, BTM = Biotite-tourmaline-muscovite, MT = Muscovite-tourmaline and Min = Mineralised pegmatites).

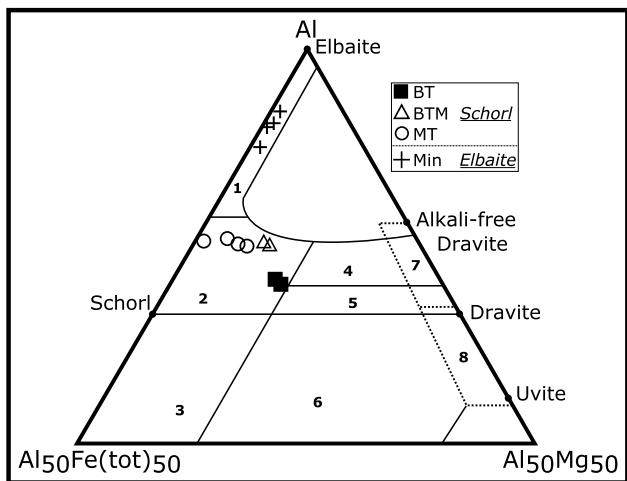


**Figure 4:** Discrimination diagram for tourmaline from different rocks, based on the Al-Fe-Mg plot (after Henry & Guidotti (1985)). 1: Li-rich granitoids, pegmatites and aplites. 2: Li-poor granitoids and their associated pegmatites and aplites. 3: Fe<sup>3+</sup>-rich quartz-tourmaline rocks (hydrothermally altered granites). 4: Metapelites and metapsammities coexisting with an Al-saturating phase. 5: Metapelites and metapsammities not coexisting with an Al-saturating phase. 6: Fe<sup>3+</sup>-rich quartz-tourmaline rocks, calc-silicate rocks, and metapelites. 7: Low-Ca metaultramafic rocks and Cr-, V-rich metasediments. 8: Metacarbonates and metapyroxenites (Schorl from BT = Biotite-tourmaline, BTM = Biotite-tourmaline-muscovite, MT = Muscovite-tourmaline and elbaite from Min = Mineralised pegmatites).

Z-site contains Al, but also significant amounts of Fe<sup>2+</sup>, Fe<sup>3+</sup>, Ti<sup>4+</sup>, Mg<sup>2+</sup>, Cr<sup>3+</sup>, V<sup>3+</sup>. On the Fe-Al-Mg classification diagram of Henry & Guidotti (1985), the apices represent the Y-site cation substitutions: Fe<sup>2+</sup> in schorl, Mg<sup>2+</sup> in dravite and (Al<sup>3+</sup>+Li<sup>+</sup>) in the elbaite series. The cation content has been related to the geological formation environment (Fig. 4; Henry & Guidotti, 1985). All the tourmalines of the schorl-dravite series plot within the field occupied by tourmaline typical from Li-poor granitoids (Fig. 4). In these tourmalines, a trend can be defined evolving from relative Mg-rich tourmalines (4.06 wt% MgO) in the innermost pegmatite zones (2 and 3), to Mg-poor schorl (1.65 wt% MgO) in muscovite-tourmaline pegmatites (zone 4). Petrographically identified elbaite tourmalines are characterised by a very low Mg content (0.05 wt% to 0.08 wt% MgO; Fig. 4), and a distinct Mn enrichment in contrast to the schorl-dravite series (Fig. 3C). The elbaite series plot in the field of Li-enriched pegmatites (Fig. 4). No major trends in Na and K content can be observed in schorl-dravite or elbaite samples. The Ti content decreases (Fig. 3D) from 0.37 wt% TiO<sub>2</sub> in schorl-dravite series of

the biotite-tourmaline (zone 2) pegmatites to 0.04 wt% in elbaite of mineralised pegmatites (zone 6 and 7). It can be concluded that the Fe-Al-Mg classification diagram clearly visualises two distinct compositional groups for tourmalines of pegmatites from the Gatumba area.

**5.2. Trace elements**

Trace elements are currently used as indicators for enrichment and differentiation processes in pegmatite systems. The elements that involve substitution in the alkali site (e.g. Rb, Cs, Sr, Ba, Pb ...) are the most thoroughly investigated. In particular, the K/Rb and K/Cs ratios in K-feldspar and muscovite-lepidolite series minerals (expressed as ppm/ppm in the text) are considered as good indicators of a pegmatite evolution (Černý et al., 1985).

**5.2.1. Feldspars**

The K/Rb ratio in K-feldspars (Fig. 5A) decreases continuously from zone 1 to zone 7, with values of 181 to 216 for biotite pegmatites (zone 1), 158 for biotite-tourmaline pegmatites (zone 2), 141 to 170 for biotite-tourmaline-muscovite pegmatites (zone 3), 41 for muscovite pegmatites (zone 5) and between 24 to 56 for mineralised pegmatites (zones 6 and 7). No K-feldspar could be sampled from muscovite-tourmaline pegmatite (zone 4). The average Rb content in zones 1, 2 and 3 is low, i.e. 350 ppm, 540 ppm and 730 ppm, respectively. Pegmatites of zone 5 and mineralised pegmatites of zones 6 and 7 display an average Rb content of 1270 ppm, 1780 ppm and 4570 ppm, respectively. Those elevated values are typical for K-feldspar from evolved pegmatite bodies (Černý et al., 1985; Neiva, 1995; Alfonso et al., 2003) and when organised according to the Varlamoff zonation pattern, the K/Rb versus Rb plot of K-feldspar describes a typical hyperbolic trend (Fig. 5A).

The K/Cs ratio of K-feldspars decreases from ~28,500 in the less evolved pegmatites of zone 1 to 2394 in highly evolved, mineralised pegmatites of zone 6 and 7 (Fig. 5B). Caesium contents are low in the zones 1, 2 and 3, with values of 2 ppm to 4 ppm, 21 ppm and 24 ppm respectively. In zone 5 and in mineralised pegmatites of zones 6 and 7, the K-feldspars contain 15 ppm up to 46 ppm Cs. Such Cs values are typical of moderately evolved pegmatites (Černý, 1994).

Although strontium and barium contents, which are currently used as indicators of the evolution in granites and pegmatites, should decrease with advancing evolution (Černý et al., 1985; Roda et al., 1999; Morteani et al., 2000), it is not the case for the minerals from pegmatites of the Gatumba area (Table 3). The Pb content of the K-feldspar decreases consistently with the K/Rb and K/Cs ratios, a trend which has been observed elsewhere (e.g. Kontak & Martin, 1997; Alfonso et al., 2003) and was even reported in a single pegmatite body (Černý & Burt, 1984).

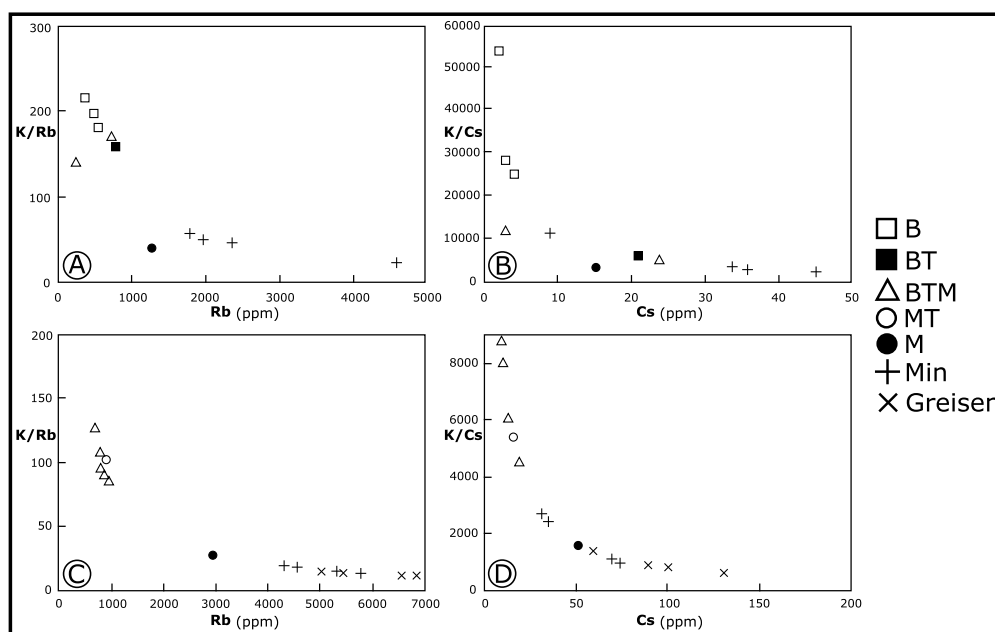


**Figure 5:** K/Rb versus Rb and K/Cs versus Cs plots of K-feldspars (A & B) and muscovites (C & D) along the zonation sequence (B = biotite, BT = Biotite-tourmaline, BTM = Biotite-tourmaline-muscovite, M = Muscovite, Min = Mineralised pegmatites). The alkali metal ratios are expressed in ppm/ppm.

Nr.	2	3	4	5	6	7	9	10	11	12	13	14	15	16	17	18	19
Zone	B	B	B	B	B	B	BT	BT	BT	BT	BT	BTM	BTM	BTM	BTM	BTM	BTM
Mineral	Bt	Or	Mc	Or	Bt	Ab	Olg	Bt	Srl	Or	Srl	Ms	Bt	Ms	Ab	Srl	Ms
Sc [0.14]	76,2	3,6	3,2	3,5	71,7	3,9	3,2	45,5	14,7	3,9	20,2	29,4	9,5	19,9	3,7	4,3	10,0
Zn [1.36]	458	3	BDL	1	472	BDL	2	514	351	1	417	22	958	69	3	477	34
Ga [0.23]	64	14	15	13	64	22	20	59	105	18	93	94	53	76	13	53	78
Ge [0.06]	4,6	2,1	2,2	2,2	5,2	2,3	2,3	4,8	2,9	5,0	3,0	2,6	5,7	2,8	3,2	4,3	5,0
Rb [0.11]	1505	540	356	483	1564	19	14	1313	BDL	776	1	671	1921	934	22	4	770
Sr [0.68]	6	69	78	68	6	86	71	11	13	85	13	7	8	2	23	7	3
Y [0.04]	1,0	1,2	0,4	0,1	2,6	1,0	0,4	2,7	BDL	0,2	0,1	0,7	43,4	14,2	4,7	0,1	BDL
Zr [0.12]	11,3	BDL	BDL	BDL	0,3	BDL	BDL	BDL	BDL	BDL	BDL	BDL	31,8	0,5	BDL	BDL	BDL
Nb [0.68]	345	BDL	BDL	BDL	379	BDL	1	372	2	BDL	2	73	359	89	BDL	2	147
Cs [0.14]	68	4	3	2	79	1	1	59	1	21	BDL	19	152	13	1	1	35
Ba [0.34]	131	660	553	637	108	22	27	184	3	468	BDL	173	114	10	19	BDL	30
Ta [0.08]	19,5	BDL	BDL	BDL	21,7	BDL	0,1	22,0	0,6	BDL	0,6	10,2	44,9	8,6	BDL	1,7	23,6
W [0.14]	8,2	0,1	BDL	BDL	1,2	BDL	0,1	3,4	BDL	BDL	0,5	13,8	3,6	15,9	BDL	0,5	34,0
Pb [0.32]	15,7	31,9	55,5	72,4	31,9	20,5	45,2	39,8	2,2	52,1	2,1	7,7	33,9	8,8	43,1	3,5	4,7
Th [0.02]	0,3	0,1	0,1	BDL	0,3	0,1	0,1	0,7	0,1	0,5	0,1	0,1	2,3	0,4	0,1	0,2	0,1
U [0.03]	10,7	0,2	0,3	0,2	18,5	0,3	0,2	2,3	0,1	0,1	0,1	0,3	9,7	1,8	0,7	0,3	0,1
Nr.	20	21	22	23	24	26	27	28	30	31	32	33	34	35	36	37	38
Zone	BTM	BTM	BTM	BTM	BTM	BTM	BTM	BTM	MT	MT	MT	M	M	Min	Min	Min	Min
Mineral	Or	Bt	Mc	Ms	Srl	Olg	Ms	Bt	Srl	Ms	Srl	Mc	Ms	Ab	Srl	Afs	Ms
Sc [0.14]	3,4	7,8	3,5	20,3	2,7	3,4	19,2	7,1	9,2	26,9	5,3	3,8	3,6	4,1	2,1	3,8	3,0
Zn [1.36]	BDL	1062	5	62	1225	2	63	1061	698	41	472	6	105	3	3125	3	107
Ga [0.23]	9	46	13	81	58	14	84	48	72	94	59	14	104	27	104	20	145
Ge [0.06]	7,5	6,3	3,0	2,5	3,7	2,9	2,7	5,9	2,4	3,6	4,1	7,2	6,0	11,0	10,0	7,0	5,8
Rb [0.11]	729	1815	231	807	7	32	840	1850	11	793	1	1270	2928	BDL	6	49	4311
Sr [0.68]	74	12	27	13	1	24	1	6	2	3	7	9	2	3	2	14	4
Y [0.04]	BDL	27,6	3,4	1,4	BDL	4,3	3,6	16,3	1,9	0,3	BDL	0,5	BDL	BDL	BDL	0,2	BDL
Zr [0.12]	BDL	28,0	BDL	BDL	BDL	BDL	2,5	55,9	21,7	BDL	BDL	BDL	BDL	BDL	30,8	BDL	9,7
Nb [0.68]	BDL	374	BDL	83	3	BDL	91	389	2	116	2	3	217	24	2	13	261
Cs [0.14]	24	134	3	9	1	1	10	144	2	16	1	15	51	BDL	1	BDL	31
Ba [0.34]	142	87	33	25	BDL	5	10	58	1	56	1	16	7	2	2	20	60
Ta [0.08]	BDL	51,5	BDL	4,6	0,5	BDL	7,0	47,6	0,4	10,6	1,7	0,7	15,0	10,5	1,2	7,5	18,8
W [0.14]	BDL	3,0	BDL	16,1	0,4	0,1	13,5	2,3	0,7	48,8	0,4	BDL	8,1	BDL	0,9	0,2	9,7
Pb [0.32]	153,7	27,2	62,3	5,6	2,2	36,0	5,8	29,6	1,1	4,9	3,7	29,0	4,5	1,3	0,9	0,7	0,8
Th [0.02]	0,1	1,7	0,3	0,1	0,1	0,2	0,2	1,4	0,7	0,1	0,2	0,1	0,2	0,1	0,1	0,3	BDL
U [0.03]	0,4	8,1	0,9	1,0	0,2	0,8	0,6	6,6	1,9	0,2	0,3	2,7	1,2	5,2	1,1	1,5	BDL
Nr.	39	40	42	43	44	45	47	48	49	50	51	52	53	55	56	58	59
Zone	Min	Min	Min	Min	Min	Min	Min	Min	Min	Min	Min	Min	Min	Gr	Gr	Gr	Gr
Mineral	Or	Ms	Ms	Ab	Or	Lpd	Ms	Elb	Elb	Elb	Elb	Mc	Afs	Ms	Ms	Ms	Ms
Sc [0.14]	3,6	3,0	3,0	3,5	3,6	2,8	3,7	2,4	1,9	2,1	2,1	3,7	3,6	2,5	2,9	2,5	2,7
Zn [1.36]	3	218	108	6	7	387	89	1103	926	1167	918	7	5	317	521	196	71
Ga [0.23]	15	150	142	23	14	71	149	104	69	110	113	12	12	82	138	83	116
Ge [0.06]	7,0	6,9	7,8	9,8	9,2	19,2	6,0	24,3	9,1	20,0	24,3	6,0	5,7	8,7	7,7	8,4	6,8
Rb [0.11]	1933	5327	5774	81	4574	16648	4573	225	9	144	231	1784	2340	5368	6986	5008	6628
Sr [0.68]	90	1	1	7	16	1	6	13	25	14	8	59	79	1	1	1	1
Y [0.04]	0,6	0,1	0,1	0,2	0,3	BDL	0,6	0,4	BDL	0,4	0,4	1,9	0,8	BDL	BDL	BDL	0,1
Zr [0.12]	BDL	BDL	BDL	13,7	BDL	8,0	BDL	BDL	BDL	BDL	BDL	26,6	13,3	BDL	BDL	0,8	BDL
Nb [0.68]	BDL	294	246	2	BDL	180	239	5	1	3	5	4	10	204	230	533	223
Cs [0.14]	9	35	69	1	34	1603	35	13	2	10	15	36	45	89	100	130	59
Ba [0.34]	659	27	36	11	268	2	94	18	2	4	7	258	166	2	1	13	2
Ta [0.08]	0,2	18,7	23,4	0,4	0,3	81,0	19,9	8,0	0,9	5,5	10,0	0,7	1,5	37,5	26,1	460,4	41,3
W [0.14]	BDL	11,0	6,9	BDL	BDL	14,5	8,5	0,4	0,5	0,4	0,3	0,7	0,3	15,9	11,2	4,1	6,1
Pb [0.32]	8,3	2,4	1,5	2,8	16,3	0,7	1,3	41,2	31,7	51,0	46,7	45,2	33,0	6,2	2,9	9,0	2,5
Th [0.02]	0,2	0,1	BDL	0,3	0,1	BDL	0,4	0,3	0,1	0,2	0,4	0,6	0,6	0,2	0,1	0,2	0,1
U [0.03]	0,1	0,5	0,1	0,2	0,1	BDL	0,3	0,7	0,3	0,7	1,2	0,4	0,2	0,1	0,1	8,8	0,1

**Table 3:** Trace element composition of the minerals from the different pegmatite zones (ICP-MS analysis); B = biotite, BT = Biotite-tourmaline, BTM = Biotite-tourmaline-muscovite, MT = Muscovite-tourmaline, M = Muscovite, Min = Mineralised pegmatites and Gr = greisens. Minerals: Afs = pink K-feldspar, Ab = albite, Bt = biotite, Elb = elbaite, Lpd = lepidolite, Mc = Microcline, Ms = muscovite, Olg = oligoclase, Or = orthoclase and Srl = schorl. (BDL = Below Detection Limit). Limit of quantification (LOQ in ppm) are reported between brackets.

In contrast with the K-feldspars, there is in general no direct relation between the trace-element contents of plagioclases and the position of the host pegmatite in the Varlamoff zonation scheme. Yet, the Rb and Cs contents are higher in zones 5, 6 and 7, relatively to zones 1, 2, 3 and 4, and the  $P_2O_5$  content increases with the degree of evolution along the Varlamoff zonation (up to 0.15 wt% in zones 1-2, 0.26 wt% in zone 3 and up to 0.47 wt% in mineralised pegmatites).

### 5.2.2. Micas

Rb and Cs contents in the muscovite-lepidolite series exhibit a progressive evolution from zone 1 to zones 6-7 and greisens (Fig. 5C-D). The K/Rb ratios vary from 127 to 12 in muscovites along the Varlamoff zonation, and lepidolite is characterised by a ratio of 5. The Rb enrichment varies from 670 ppm in muscovites from non-mineralised pegmatites of zones 4 and 5, up to 6986 ppm in muscovites of both mineralised pegmatites and greisens, and 16,648 ppm in lepidolite. The K/Cs ratio decreases from 8995 to 613 in muscovite, and amounts to 52 in lepidolite. The absolute Cs content varies from 8 ppm to 130 ppm in muscovite along the zonation, and to 1602 ppm in lepidolite. The secondary muscovites from the greisens form an intrinsic part of the Rb and

Cs enrichment trends and, as such, overlap with the muscovites from the mineralised pegmatites. Barium and strontium exhibit a broad range of values in these pegmatites, without any obvious correlation with the pegmatite zonation.

The K/Rb and K/Cs ratios of biotites are respectively between 50-37 and 1100-340. Total concentrations vary between 1300 ppm and 1930 ppm Rb, and 60 ppm and 152 ppm Cs. The enrichment is consistent with the zonation sequence. The Ba content of biotite exhibits a decrease along the Varlamoff zonation from 185 ppm to 60 ppm. The Sr content varies between 6 ppm and 12 ppm but without correlation with the pegmatite zonation.

## 6. Discussion

### 6.1. Geochemical zonation sequence

Biotites are characterised by an increase of the  $Fe_{tot}/(Fe_{tot}+Mg)$  ratio and a decrease in the Mg, Mn and Ti content along the Varlamoff zonation. In general, the transition metals Mn, Fe, Ti, but also Mg, are highly compatible elements in biotite (Nash & Crecraft, 1985; Icenhower & London, 1995). Consequently,

an increase in their content in biotites is expected as a result of differentiation. This is, however, not the case for the Gatumba area biotites. This may be due to the overall high fraction of biotite (~15%; and consequently bulk distribution coefficients for Fe, Ti, Mn and Mg greater than unity) in the innermost, biotite-bearing pegmatites as well as to the co-crystallisation of schorl together with biotite; as schorl expresses a corresponding compatible behaviour for the transition metals (Fe and Ti) and Mg. Biotites studied by Lentz (1992) from rare-element pegmatites in the southwestern Grenville Provinces (Canada) also display an increase of the  $Fe_{tot} / (Fe_{tot} + Mg)$  ratio according to the differentiation trend of the pegmatite system. Tourmaline, however, is rarely observed in the pegmatite system described by Lentz (1992), therefore the biotites show a tendency to higher Ti content along the differentiation trend of the pegmatite system.

The observed variation in tourmaline solid-solution that forms two distinct compositional groups (see 5.1.3.), helps to define the regional fractionation trend of the Gatumba pegmatite field. Tourmaline fractionation in the Gatumba area is observed firstly on a group-scale. The black tourmalines of group 1 express an evolution from Mg-rich schorl in biotite-tourmaline pegmatites (zone 2) to nearly end-member composition, Mg-poor schorl in muscovite-tourmaline pegmatites (zone 4). Group 2 tourmalines are characterised by the stabilisation of an elbaite phase with an increased Mn content in the mineralised pegmatites of zones 6 and 7. Both tourmaline groups 1 and 2 are, however, compositionally separated and no continuous evolution trend is observed between both groups. The abrupt compositional transition of group 1 to group 2 tourmalines may be interpreted to reflect an evolution of the pegmatitic melt composition. Boron is highly incompatible in all rock-forming minerals, except tourmaline (Grew, 2002). With increasing chemical fractionation of the pegmatitic melt, the composition of tourmaline evolves from dravite- to schorl-rich, hence the stability of schorl hinges mostly on mafic components such as Fe, Mg and Ti (i.e. boron cycle; London, 2008). Due to the combined crystallisation of schorl and biotite in the early biotite-tourmaline rich pegmatites, the activities of Fe, Ti and Mg are lowered in the melt causing the destabilisation of tourmaline (Le Châtelier's principle; Wolf & London, 1997), which in turn hampers the regulation of the B content of the melt. As such, the combined crystallisation of schorl and biotite effectively consumes the mafic components of the melt and induces cessation of the schorl tourmaline crystallisation (common tourmaline cessation observed by Wolf & London, 1997; London, 2008). The mafic component drop also hampers the biotite stability and promotes the growth of muscovite. The evolution from schorl to elbaite is paragenetically separated by a transient cessation of tourmaline crystallisation, which allowed an increase of the B content of the melt due to fractionation (cf. London, 2008). Fractionation also raised the incompatible Li content to the level required to stabilise the formation of elbaite.

A general decrease of Mn in tourmalines along the Varlamoff zonation would be expected in relation to the proposed declining fractionation trend of Mn in biotites. Indeed, the Mn content of schorl tourmalines declines along the Varlamoff zonation (0.18 wt% in zone 2 to 0.08 wt% MnO in zone 5). Varlamoff (1954a) also reported garnets of the pyralisite solid solution series in the innermost pegmatites of zones 1 and 2 (Table 1). So biotite and garnet can be held responsible for the depletion of Mn in the initial melt (crystallising the biotite- and biotite-muscovite-bearing pegmatites) due to their overall high Mn partition coefficients (London et al., 2001). In contrast elbaite shows high Mn contents with respect to schorl, which is due to the exceptional compatible behaviour of Mn in Li-rich tourmalines (London et al., 2001).

The observed compositional variation of tourmaline implies that the 7-zones mineralogical zonation of Varlamoff (1954a) can be simplified to a regional zonation that only involves 4 zones, by omitting tourmaline from the classification. This results in a biotite, a 2-mica, a muscovite and a mineralised zone. The schorl tourmalines belong in terms of a geochemical evolution of the Gatumba pegmatite melt (i.e. boron cycle; London, 2008) to the same group. Their compositional differences are solely defined by the fractionation processes of the melt. The simplified classification also groups the zones 6 and 7 mineralised pegmatites

as one group. The detailed and state-of-the-art classification by Dewaele et al. (2011) already incorporated these evolved pegmatites as LCT-family, rare-element class pegmatites based on their petrogenetic-geochemical signatures.

## 6.2. Alkali metal fractionation

The evolution of the total concentration of alkali metals and their ratios (K/Rb and K/Cs) of both K-feldspars and micas provide good evidence for the chemical fractionation among the pegmatites of the Gatumba area. The fractionation behaviour in the melt is mainly based on the compatibility of these alkali metals. Rb is compatible in micas (muscovite, biotite and lepidolite), weakly incompatible in K-feldspars and incompatible in plagioclase (London, 2008). Micas and feldspars are the principle reservoir for Cs (London, 2005b). The observation that the Rb and Cs levels rise uniformly for all mineral separates of K-feldspar and muscovite-lepidolite throughout the regional pegmatite zonation sequence points to two important factors: (1) the distribution coefficients of both Rb as Cs have to be less than unity for the Gatumba pegmatite system, so that these incompatible elements can become enriched in the melt with advancing fractionation; (2) a profound fractionation of the pegmatitic melt is essential to increase the alkali metal content, e.g. in the case of K-feldspars up to a factor of 20 for Rb and 25 for Cs. The Rb and Cs contents of muscovite increase with a factor of 10 and 16 respectively and of lepidolite with a factor of 25 for Rb and 200 for Cs. Fractional crystallisation and subsequent enrichment of incompatible elements (cf. Hanson, 1978) appear to be the principal mechanism by which the trace-element signatures are modified once the melt is separated from its source G4-granite and gave rise to the observed regional pegmatite zonation in the Gatumba area.

It should be noted that the Rb and Cs content of lepidolite and greisen muscovites, which are interpreted to be secondary in origin, demonstrate an enriched chemical signature that corresponds to their paragenetic appearance in the zonation sequence. Both micas are replacement assemblages after (K)-feldspar of mineralised pegmatites. It is generally agreed that lepidolite-rich units are among the latest units to consolidate and they are largely interpreted as subsolidus, metasomatic assemblages. However, some authors still consider the possibility of precipitation from exsolved immiscible liquid or the solidification from a residual magma (discussion in Černý et al., 1985). No evidence has been found which points to a primary solidification origin of lepidolite in the Gatumba area. In contrary, muscovite in greisens is undoubtedly a hydrothermal-metasomatic product, replacing the primary pegmatitic mineral assemblages. To conclude, the late greisen muscovites and lepidolite replacing feldspar seem to inherit their total Rb and Cs content as well as the K/Rb and K/Cs ratios of their enriched feldspar precursors.

The behaviour of Sr and Ba among the Gatumba pegmatite zonation shows less systematic variation than might be expected according to Černý et al. (1985). London (2008 and references therein) also observed a random behaviour of these alkali earth metals and considered that (1) external sources of Ba and Sr, (2) retention of Ba and Sr by fluxed magmas, and (3) the systematic differences in the partitioning of both elements among plagioclase, K-feldspar and melt could cause the variable Sr and Ba content. Breiter et al. (1999) also observed a random distribution of Sr in Sn-W mineralised pegmatites of the Erzgebirge. These authors reported that the Sr redistribution was caused by highly reactive aqueous solution responsible for pervasive greisenisation and feldspathisation. Consequently, these reported element redistribution processes may be important in the evolution of the Gatumba pegmatite field, due to the magnitude of metasomatic alteration features in the mineralised pegmatites by late H<sub>2</sub>O-CO<sub>2</sub>-NaCl-KCl fluids (Dewaele et al., 2008).

## 6.3. Origin of the Gatumba pegmatite field

Field, mineralogical and geochemical criteria indicate that the pegmatites from the Gatumba area show characteristics similar to many rare-element pegmatite fields (cf. Černý, 1991; Simmons & Webber, 2008). (1) Mineralogical and geochemical features become more complex as one moves in northwest direction through the pegmatite field starting from the biotite pegmatites at the margin of the Gitarama pluton (Fig. 2). (2) The most evolved,

mineralised pegmatites are affected by hydrothermal/metasomatic alteration: albitisation, sericitisation and muscovitisation (i.e. greisenisation), as proposed by e.g. Kontak (2006). (3) Some minerals are restricted to specific pegmatite zones (Table 1), e.g. (a) tourmaline changes composition with increasing distance in the zonation sequence. Schorl in innermost, barren pegmatite zones evolves to elbaite in outermost, mineralised pegmatites. (b) Lepidolite is restricted to the mineralised pegmatites. (c) Columbite-tantalite and cassiterite are generally restricted to the most evolved mineralised zones. (4) A regional zonation is not only reflected in the mineral evolution of the pegmatites but also in the chemical composition of the main minerals: (a) biotite and tourmaline show a general decrease in mafic components along the zonation (e.g. Fe, Mg and Ti). The  $Fe_{tot} / (Fe_{tot} + Mg)$  ratio of these minerals increases parallel to the zonation. (b) The K/Rb and K/Cs ratio of feldspar and muscovite decrease along the zonation, which is in agreement with a trend of increasing fractionation observed by other authors (Černý, 1985; Mulja et al., 1995; London, 2008).

All these data suggest that the pegmatites from the Gatumba area are the result of the same petrogenetic process. As such, the substantial chemical fractionation in the regional Gatumba pegmatite field accompanies the evolution from common pegmatites (biotite, 2-mica and muscovite pegmatites) to rare-element pegmatites (mineralised pegmatites). The K/Rb versus Rb data in Fig. 5 seem to show a hiatus between the common pegmatites (biotite, 2-mica and muscovite pegmatites) and the mineralised pegmatites, which could alternatively be interpreted as reflecting two independent fractionation trends. Roda et al. (1999) interpreted the regional zonation observed in the Fregeneda area (Spain) to be the result of at least three different paths of fractional crystallisation of granitic melts generated by various degrees of partial melting of metasediments. Indeed, these authors show good evidence for the existence of multiple fractionation trends: (1) the observation of crosscutting relationships between highly evolved pegmatites from different paragenetic zones. (2) The most outwardly pegmatite zone of the Fregeneda area only shows intermediate K/Rb and K/Cs ratios. So, they show inconsistent fractionation behaviour compared to a standard pegmatite evolution sequence (i.e. single path of fractional crystallisation). Various degrees of partial melting resulted in different melt batches with different degrees of trace element enrichments, which in turn generated the varying compositional evolution of the Fregeneda pegmatites (Roda et al., 1999). In the Gatumba area, no crosscutting relationships are observed between pegmatites representative of the different zones and the pegmatite spatial distribution fits well with the chemical composition of their minerals (Figs 2 & 5). The hiatus is thought to be caused by the few (3) feldspar and muscovite separates from the muscovite pegmatites (see 5.2.).

London (2008 and references therein) suggested three end-member mechanisms of regional zonation in a pegmatite field. A first scenario involves a sequential and pulsed tapping from an evolving pluton. This scenario can be excluded for the Gatumba area since this sequential tapping would imply cross-cutting relations between the dikes of different zones, which is not recognised in field. A second scenario, which is based on the simultaneous chemical fractionation in an open system over the entire distance of the pegmatite complex, is also unlikely. The different pegmatite zones of the Gatumba area demonstrate a single path of geochemical evolution based on various mineralogical and geochemical proxies. In addition, the field relationships indicate that the pegmatite dikes are not a continuous feature. The pegmatites occur as individual dikes ("necking down") with various dimensions and a clear and unique mineralogical composition (cf. Varlamoff zonation). Consequently, an open system fractionation can be excluded because this scenario would require that the distal pegmatite-forming melts remain interconnected with the main body of the granite throughout the entire time period of pegmatite formation. The most likely scenario for the Gatumba area involves a third scenario proposed by London (2008): the existence of an already vertical zonation within the G4 source pluton by fractional crystallisation, as schematically represented in Fig. 6 (cf. Hildreth, 1979; Michael, 1983; Bea et al., 1994; Mulja et al., 1995; London, 2005b). The

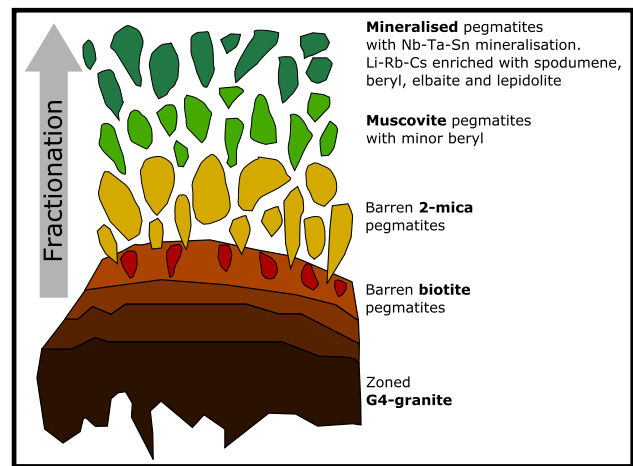


**Figure 6:** Schematic representation of the compositional evolution along the newly defined zonation (according to the representation of London, 2008). Field and geochemical data of the pegmatite zonation point to the existence of a chemical zonation within the granite magma chamber prior to the pegmatite emplacement. The pegmatite zones become gradual enriched in incompatible elements due to fractionation: starting with Be (beryl), Li (spodumene, elbaite, lepidolite ...), Rb-Cs (in feldspars and muscovite-lepidolite series), Nb-Ta (columbite-tantalite mineralisation) and Sn (cassiterite mineralisation) outward from a G4-granite. The colour code, which is applied to the different pegmatites zones, is similar to Fig. 2.

crystallisation history of a rare-element-enriched granitic magma and the formation of regional zoned LCT-family pegmatites have been documented in detail by e.g. Černý (1991), Breaks & Moore (1992), Mulja et al. (1995), London (2005b), Selway et al. (2005) and Kontak (2006). Mulja et al. (1995) pointed out that a process such as early side-wall crystallisation of an initial biotite monzogranite melt and continued fractional crystallisation produce a chemically-zoned pluton with successive differentiated melt compositions (two-mica and muscovite monzogranite compositions). Late-stage expulsion of a volatile-rich melt from the magma chamber owing to fluid overpressure, and further expulsion of the highly-evolved pegmatitic melts by pluton contraction due to advancing crystallisation and cooling, resulted in the observed pegmatite zonation (Mulja et al., 1995). Striking mineralogical similarities between the barren, common pegmatites (biotite, 2-mica and muscovite zones) of the Gatumba area with the early-developed melt compositions (biotite, two-mica and muscovite monzogranite compositions) observed by Mulja et al. (1995) could point to similar processes responsible for expulsion and differentiation of the evolved pegmatitic melt associated with a chemically zoned G4-granite in the Gatumba area.

## 7. Conclusion

Mineral separates of feldspar, biotite, muscovite and tourmaline representing the whole pegmatite range of the regional zonation and alteration in the Gatumba pegmatite field have been analysed for major, minor and trace elements in order to determine the evolution of the pegmatites and the mineralogical zonation in terms of geochemical differentiation.

Tourmaline from different pegmatite zones shows significant compositional variation. The crystallisation of schorl and biotite consumed Fe and Mg to the extent that the mafic components of the pegmatitic melt dropped to trace levels. This hampered their stability and promoted the growth of muscovite. The green elbaite variant of tourmaline is restricted to the highly evolved pegmatitic quartz core of mineralised pegmatites. The evolution from schorl to elbaite has been shown to be paragenetically separated by a transient cessation of tourmaline crystallisation, which allowed for an increase of the B content of the melt due to fractionation. Fractionation also raised the Li content to the level needed to stabilise the formation of elbaite. The compositional variation of tourmaline implies that the zonation of Varlamoff (1954a)

with 7 zones can be simplified to one involving only 4 zones: biotite, two-mica, muscovite and mineralised.

Alkali element variations (K-Rb-Cs) in muscovite and K-feldspar indicate that the origin of the different pegmatite zones can be explained by a single path of fractional crystallisation of a granitic melt. Main and trace element variations in minerals from the different pegmatite zones show an evolutionary path from the biotite pegmatites to the Nb-Ta-Sn mineralised pegmatites and alteration assemblages located at the outermost part of the field. This differentiation trend reflects the increasingly more fractionated melt composition and the systematic enrichment of the incompatible trace elements Li, Rb and Cs according to the newly defined zonation. Trace element analysis on the late, secondary greisen muscovites and lepidolite, which replaced K-feldspar, inherited the alkali metal content of their enriched precursor.

Finally, we propose a pegmatite zonation model that combines the field observations of the granite-pegmatite system with a single path of extreme fractional crystallisation. The Gatumba area mineralised pegmatites represent the last small fraction of melt remaining after granite fractionation in a chemically zoned pluton with G4-affinity.

## 8. Acknowledgements

Research of Niels Hulsbosch is funded by a Ph.D. grant of the Agency for Innovation by Science and Technology (IWT). We would like to express our gratitude to dr. Elvira Vassilieva for her help with the ICP-OES analyses, Herman Nijs for preparing the thin sections and dr. Friso De Clercq for the valuable information on the geology and metallogenesis of Rwanda. We would also like to thank Jacques Navez and Laurence Monin of the RMCA for the assistance with the ICP-QMS analyses. Prof. Jean-Clair Duchesne is thanked for the editorial handling of the manuscript. Prof. Christian Marignac and an anonymous reviewer are acknowledged for the careful review of the text.

## 9. References

- Alfonso, A.P., Melgarejo, J.C., Yusta, I. & Velasco, F., 2003. Geochemistry of feldspars and muscovite in granitic pegmatite from Cap de Creus field, Catalonia, Spain. *The Canadian Mineralogist*, 41, 103–116.
- Baudet, D., Hanon, M., Lemonne, E. & Theunissen, K., 1988. Lithostratigraphie du domaine sédimentaire de la chaîne Kibarienne au Rwanda. *Annales de la Société Géologique de Belgique*, 112, 225–246.
- Bea, F., Pereira, M.D., Corretgé, L.G. & Fershtater, G.B., 1994. Differentiation of strongly peraluminous, perphosphorous granites. The Pedrobernardo pluton, central Spain. *Geochimica et Cosmochimica Acta*, 58, 2609–2628.
- Beurlen, H., De Moura, O.J.M., Soares, D.R., Da Silva, M.R.R. & Rhede, D., 2011. Geochemical and geological controls on the genesis of gem-quality “Paraíba Tourmaline” in granitic pegmatites from northeastern Brazil. *The Canadian Mineralogist*, 49, 277–300.
- Breaks, F.W. & Moore, J.M., 1992. The Ghost Lake Batholith, Superior Province of Northwestern Ontario: A fertile, S-type, peraluminous granite-Rare element pegmatite system. *The Canadian Mineralogist*, 30, 835–875.
- Breiter, K., Förster, H.-J. & Seltsmann, R., 1999. Variscan silicic magmatism and related tin-tungsten mineralization in the Erzgebirge-Slavkovský les metallogenic province. *Mineralium Deposita*, 34, 505–521.
- Brinckmann, J. & Lehmann, B., 1983. Exploration de la bastnaésite-monacite dans la région de Gakara, Burundi. Unpublished Report, Bujumbura/Hannover, 157 pp.
- Brinckmann, J., Lehmann, B. & Timm, F., 1994. Proterozoic gold mineralisation in NW Burundi. *Ore Geology Reviews* 9, 85–103.
- Brown, C.D. & Wise, M.A., 2001. Internal zonation and chemical evolution of the Black Mountain granitic pegmatite, Maine. *The Canadian Mineralogist*, 39, 45–55.
- Cahen, L. & Snelling, N.J., 1966. *The Geochronology of Equatorial Africa*. North-Holland Publishing Company, Amsterdam, 200 pp.
- Cahen, L., Snelling, N.J., Delhal, J., Vail, J.R., Bonhomme, M. & Ledent, D., 1984. *The geochronology and evolution of Africa*. Oxford University Press, Oxford, 512 pp.
- Černý, P., 1991. Rare-element granitic pegmatites. Part 1: Anatomy and internal evolution of pegmatite deposits. Part 2: Regional to global environments and petrogenesis. *Geoscience Canada*, 18, 49–81.
- Černý, P., 1994. Evolution of feldspars in granitic pegmatites. In Parsons, I. (ed.), *Feldspars and Their Reactions*. NATO ASI Series C, 501–540.
- Černý, P. & Burt, D.M., 1984. Paragenesis, crystallochemical characteristics, and geochemical evolution of micas in granitic pegmatites. In Bailey, S.W. (ed.), *Micas. Reviews in Mineralogy and Geochemistry*, 13, 257–297.
- Černý, P. & Ereit, T.S., 2005. The classification of granitic pegmatites revisited. *The Canadian Mineralogist*, 43, 2005–2026.
- Černý, P., Meintzer, R.E. & Anderson, A.J., 1985. Extreme fractionation in rare element granitic pegmatites: selected examples of data and mechanism. *The Canadian Mineralogist*, 23, 381–421.
- De Clercq, F., Muchez, Ph., Dewaele, S. & Boyce, A., 2008. The tungsten mineralisation at Nyakabingo and Gifurwe (Rwanda): preliminary results. *Geologica Belgica*, 11, 251–258.
- De Clercq, F., 2012. *Metallogenesis of the Nb-Ta, Sn and W ore deposits in the northern Kibara belt (Rwanda)*. Unpublished doctoral dissertation, KU Leuven, Belgium.
- Dewaele, S., Tack, L., Fernandez, M., Boyce, A. & Muchez, Ph., 2007a. Cassiterite and columbite-tantalite mineralisation in pegmatites of the northern part of the Kibara orogen (Central Africa): the Rutongo area (Rwanda). *Proceedings of the 9th Biennial SGA Meeting. Mineral Exploration and Research: Digging Deeper 20th-23rd August 2007*, Dublin, Ireland, 1489–1492.
- Dewaele, S., Tack, L., Fernandez, M., Boyce, A. & Muchez, Ph., 2007b. Cassiterite mineralisation in vein-type deposits of the Kibara orogen (Central Africa): Nyamiumba Rutongo area, Rwanda). *Proceedings of the 9th Biennial SGA Meeting. Mineral Exploration and Research: Digging Deeper 20th-23rd August 2007*, Dublin, Ireland, 1007–1010.
- Dewaele, S., Tack, L., Fernandez-Alonso, M., Boyce, A., Muchez, Ph., Schneider, J., Cooper, G. & Wheeler, K., 2008. Geology and mineralisation of the Gatumba area, Rwanda: present state of knowledge. *Etudes Rwandaises*, 16, 6–24.
- Dewaele, S., Tack, L. & Fernandez, M., 2009. Cassiterite and columbite-tantalite (coltan) mineralisation in the Mesoproterozoic rocks of the northern part of the Kibara orogen (Central Africa): preliminary results. *Mededelingen der Zittingen van de Koninklijke Academie voor Overzeese Wetenschappen*, 54, 341–357.
- Dewaele, S., De Clercq, F., Muchez, P., Schneider, J., Burgess, R., Boyce, A. & Fernandez-Alonso, M., 2010. Geology of the cassiterite mineralisation in the Rutongo Area, Rwanda (Central Africa): current state of knowledge. *Geologica Belgica*, 13, 91–112.
- Dewaele, S., Henjes-Kunst, S., Melcher, F., Sitnikova, M., Burgess, R., Gerdes, A., Fernandez-Alonso, M., De Clercq, F., Muchez, Ph. & Lehmann, B., 2011. Late Neoproterozoic overprinting of the cassiterite and columbite-tantalite bearing pegmatites of the Gatumba area, Rwanda (Central Africa). *Journal of African Earth Sciences*, 61, 10–26.
- Fernandez-Alonso, M., Lavreau, J. & Klerkx, J., 1986. Geochemistry and geochronology of the Kibaran granites in Burundi, Central Africa: implication for the Kibaran orogeny. *Chemical Geology*, 57, 217–234.
- Fernandez-Alonso, M., Cutten, H., De Waele, B., Tack, L., Tahon, A., Baudet, D. & Barrit, S. D., 2012. The Mesoproterozoic Karagwe-Ankole Belt (formerly the NE Kibara Belt): The result of prolonged extensional intracratonic basin development punctuated by two short-lived far-field compressional events. *Precambrium Research*, 216, 63–86.
- Fersmann, A., 1931. Über die geochemisch-genetische Klassifikation der Granitpegmatite. *Mineralogische und Petrographische Mitteilungen* 41, 64–83.
- Fisher, D.J., 1968. Albite variant cleavelandite, and the signs of its optic directions. *The American Mineralogist*, 53, 1568–1578.
- Gérards, J., 1965. Géologie de la région de Gatumba. *Bulletin du Service Géologique Rwandaise*, 2, 31–42.
- Gérards, J. & Ledent, D., 1970. Grands traits de la géologie du Rwanda, différents types de roches granitiques et premières données sur les âges de ces roches. *Annales de la Société Géologique de Belgique*, 93, 477–489.
- Grew, E.S., 2002. Borosilicates (exclusive of tourmaline) and boron in rock-forming minerals in metamorphic environments. In Grew, E.S. & L.M. Anovitz, L.M. (eds), *Boron: Mineralogy, Petrology, and Geochemistry. Reviews in Mineralogy*, 33, 389–502.
- Günther, M.A., 1990. Flüssigkeitseinschlüsse und geologisches Umfeld zentralafrikanischer Sn-, W- und Au-Lagerstätten (Rwanda und Burundi). Unpublished doctoral dissertation, Naturwissenschaftlichen Fakultät der technischen Universität Carolo-Wilhelmina zu Braunschweig, 144 pp.
- Hanson, G.N., 1978. The application of trace elements to the petrogenesis of igneous rocks of granitic composition. *Earth and Planetary Science Letters*, 38, 26–43.

- Hawthorne, F.C. & Černý, P., 1982. The mica group. Mineralogical Association of Canada Short Course Handbook 8, 63-98.
- Hawthorne, F.C. & Henry, D.J., 1999. Classification of the minerals of the tourmaline group. *European Journal of Mineralogy*, 11, 201-215.
- Henry, D.J. & Guidotti, C.V., 1985. Tourmaline as a petrogenetic indicator mineral: an example from the staurolite-grade metapelites of NW Maine. *The American Mineralogist*, 70, 1-15.
- Hildreth, W., 1979. The Bishop Tuff: evidence for the origin of compositional zonation in silicic magma chambers. In Chapin, C.E. & Elston, W.E. (eds), *Ash-Flow Tuffs*. Geological Society of America, Special Paper, 180, 43-75.
- Icenhower, J. & London, D., 1995. Experimental partitioning of Rb, Cs, Sr, and Ba between alkali feldspar and peraluminous melt. *The American Mineralogist*, 81, 719-734.
- Jolliff, B.L., Papike, J.J., & Shearer, C.K., 1987. Fractionation trends in mica and tourmaline as indicators of pegmatite internal evolution: Bob Ingersoll pegmatite, Black Hills, South Dakota. *Geochimica et Cosmochimica Acta*, 51, 519-534.
- Kontak, D.J., 2006. Nature and origin of an LCT-suite pegmatite with late-stage sodium enrichment, Brazil Lake, Yarmouth County, Nova Scotia. I. Geological settings and Petrology. *The Canadian Mineralogist*, 44, 563-598.
- Kontak, D.J. & Martin, R.F., 1997. Alkali feldspar in the peraluminous South Mountain batholith, Nova Scotia: trace element data. *The Canadian Mineralogist*, 35, 959-977.
- Lehmann, B., Melcher, F., Sitnikova, M.A. & Rzindana Munana, J., 2008. The Gatumba rare metal pegmatites: chemical signature and environmental impact. *Etudes Rwandaises*, 16, 25-40.
- Lentz, D., 1992. Petrogenesis and geochemical composition of biotites in rare-element granitic pegmatites in the southwestern Grenville Province, Canada. *Mineralogy and Petrology*, 46, 239-256.
- Linnen, R.L. & Cuney, M., 2005. Granite-Related Rare-Element Deposits and Experimental Constraints on Ta-Nb-W-Sn-Zr-Hf Mineralization. In Linnen, R.L. & Samson, I.M. (eds), *Rare-Element Geochemistry and Mineral Deposits*, Geological Association of Canada, GAC Short Course Notes 17, 45-68.
- London, D., 2005a. Granitic pegmatites: an assessment of current concepts and directions for the future. *Lithos*, 80, 281-303.
- London, D., 2005b. Geochemistry of alkalis and alkaline earths in ore-forming granites, pegmatites, and rhyolites. In: Linnen, R. and Sampson, I. (eds), *Rare-element geochemistry of ore deposits 17*. Geological Association of Canada Short Course Handbook, 17-43.
- London, D., 2008. Pegmatites. Mineralogical Association of Canada, Québec, Canada. 347 pp.
- London, D., Evensen, J.M., Fritz, E., Icenhower, J.P., Morgan, G.B. & Wolf, M.B., 2001. Enrichment and accommodation of manganese in granite-pegmatite systems. 11Th Annual Goldschmidt Conference Abstract 3369, Lunar Planetary Institute Contribution 1088, Lunar Planetary Institute, Houston (CD-ROM).
- Melcher, F., Graupner, T., Henjes-Kunst, F., Oberthür, T., Sitnikova, M., Gäbler, E., Gerdes, A., Brätz, H., Davis, D. & Dewaele, S., 2008a. Analytical Fingerprint of Columbite-Tantalite (Coltan). Mineralisation in Pegmatites – Focus on Africa. AusIMM Ninth International Congress for Applied Mineralogy Brisbane, QLD, 8-10 September 2008, 615-624.
- Melcher, F., Sitnikova, M., Graupner, T., Martin, N., Oberthür, T., Henjes-Kunst, F., Gäbler, E., Gerdes, A., Brätz, H., Davis, D. & Dewaele, S., 2008b. Fingerprinting of conflict minerals: columbitetantalite ("coltan") ores. *SGA News*, 23.
- Melcher, F., Graupner, T., Sitnikova, M., Henjes-Kunst, F., Oberthür, T., Gäbler, H.-E., Bahr, A., Gerdes, A., Brätz, H. & Rantitsch, G., 2009a. Ein Herkunftsnachweis für Niob-Tantal-erze am Beispiel afrikanischer Selten-Element-Pegmatite. *Mitteilungen der Österreichischen Mineralogischen Gesellschaft*, 155, 231-267.
- Melcher, F., Graupner, T., Sitnikova, M., Oberthür, T., Gäbler, H.-E., Bahr, A. & Henjes-Kunst, F., 2009b. Herkunftsnachweis von Columbit-Tantalit-Erzen Status-quo-Bericht. *Tagebuch Nr.: 11082/09*. Unpublished Report Bundesanstalt für Geowissenschaften und Rohstoffe, Hannover.
- Michael, P.J., 1983. Chemical differentiation of the Bishop Tuff and other high-silica magmas through crystallization processes. *Geology*, 11, 31-34.
- Montel, J.-M., 1993. A model for monazite / melt equilibrium and application to the generation of granitic magmas. *Chemical Geology*, 110, 127-146.
- Morteani, G., Preinfalk, C. & Horn, A.H., 2000. Classification and mineralization potential of the pegmatites of the Eastern Brazilian Pegmatite Province. *Mineralium Deposita*, 35, 638-655.
- Mulja, T., Williams-Jones, A.E., Wood, S.A. & Boily, M., 1995. The Rare-element-enriched monzogranite-pegmatite-quartz vein systems in the Preissac-Lacorne Batholith, Quebec. II. Geochemistry and Petrogenesis. *The Canadian Mineralogist*, 33, 817-833.
- Nash, W.P. & Crecraft, H.R., 1985. Partition coefficients for trace elements in silicic magmas. *Geochimica et Cosmochimica Acta*, 49, 2309-2322.
- Neiva, A.M.R., 1995. Distribution of trace elements in feldspars of granitic aplites and pegmatites from Alijó-Sanfins, northern Portugal. *Mineralogical Magazine*, 59, 35-45.
- Novák, M. & Černý, P., 1998. Abundance and fractionation trends of Rb and Cs in micas from lepidolite- and elbaite-subtype pegmatites in the Moldanubicum, Czech Republic. *Acta Universitatis Carolinae: Geologica*, 42, 86-90.
- Pohl, W., 1994. Metallogeny of the northeastern Kibara belt, Central Africa – recent perspectives. *Ore Geology Reviews*, 9, 105-130.
- Pohl, W., 2011. *Economic Geology Principles and Practice: Metals, Minerals, Coal and Hydrocarbons - Introduction to Formation and Sustainable Exploitation of Mineral Deposits*, Blackwell Publishing, 663 pp.
- Pohl, W. & Günther, M.A., 1991. The origin of Kibaran (late Mid-Proterozoic) tin, tungsten and gold quartz vein deposits in Central Africa: a fluid inclusion study. *Mineralium Deposita*, 26, 51-59.
- Roda, E., Pesquera, A., Velasco, F. & Fontan, F., 1999. The granitic pegmatites of the Fregeneda area (Salamanca, Spain): characteristics and petrogenesis. *Mineralogical Magazine*, 63, 535-558.
- Roda, E., Keller, P., Pesquera, A., & Fontan, F., 2007. Micas of the muscovite-lepidolite series from Karibib pegmatites, Namibia. *Mineralogical Magazine*, 71, 41-62.
- Selway, J.B., Breaks, F.W. & Tindle, A.G., 2005. A Review of Rare-Element (Li-Cs-Ta) Pegmatite Exploration Techniques for the Superior Province, Canada, and Large Worldwide Tantalum Deposits. *Exploration and Mining Geology*, 14, 1-30.
- Simmons, W.B. & Webber, K.L., 2008. Pegmatite genesis: state of the art. *European Journal of Mineralogy* 20, 421-438.
- Štemprok, M., 1987. Greisenization (a review). *Geologische Rundschau*, 76, 169-75.
- Suhr, N.H. & Ingamells, C.O., 1966. Solution technique for the analysis of silicates. *Analytical chemistry*, 38, 730-734.
- Tack, L., Wingate, M.T.D., De Waele, B., Meert, J., Belousova, E., Griffin, B., Tahon, A. & Fernandez-Alonso, M., 2010. The 1375 Ma 'Kibaran event' in Central Africa: Prominent emplacement of bimodal magmatism under extensional regime. *Precambrian Research*, 180, 63-84.
- Tobi, A.C. & Kroll, H., 1975. Optical determination of the An-content of plagioclases twinned by Carlsbad-law: a revised chart. *American Journal of Science*, 275, 731-736.
- Varlamoff, N., 1954a. Répartition des types de pegmatites autour de la partie nord-ouest du grand massif granitique de Nyanza. *Annales de la Société Géologique de Belgique*, 78, 1-21.
- Varlamoff, N., 1954b. Tendances actuelles dans l'étude des pegmatites à travers le monde; revue des travaux sur les pegmatites du Congo belge et du Ruanda-Urundi; proposition d'une classification des pegmatites du Congo belge et de Ruanda-Urundi. *Annales de la Société Géologique de Belgique*, 77, 245-267.
- Varlamoff, N., 1956. Transitions entre les pegmatites et les filons de quartz dans les massifs granitiques des régions stannifères du Maniema (Congo belge). *Annales de la Société Géologique de Belgique*, 79, 385-403.
- Varlamoff, N., 1961. Pegmatites à amblygonite et à spodumène et pegmatites fortement albitisées à spodumène et à cassitérite de la région de Katumba (Ruanda). *Annales de la Société Géologique de Belgique*, 84, 257-278.
- Varlamoff, N., 1963. Les phénomènes de greisenification, d'albitisation et de lépidolisation et leurs relations spatiales avec les granites et les pegmatites granitiques d'Afrique. *Annales de la Société Géologique de Belgique*, 86, 285-322.
- Varlamoff, N., 1972. Central and West African Rare-Metal Granitic Pegmatites, Related Aplites, Quartz Veins and Mineral Deposits. *Mineralium Deposita*, 7, 202-216.
- Wolf, M.B. & London, D., 1997. Boron in granitic magmas: stability of tourmaline in equilibrium with biotite and cordierite. *Contributions to Mineralogy and Petrology*, 130, 12-30.

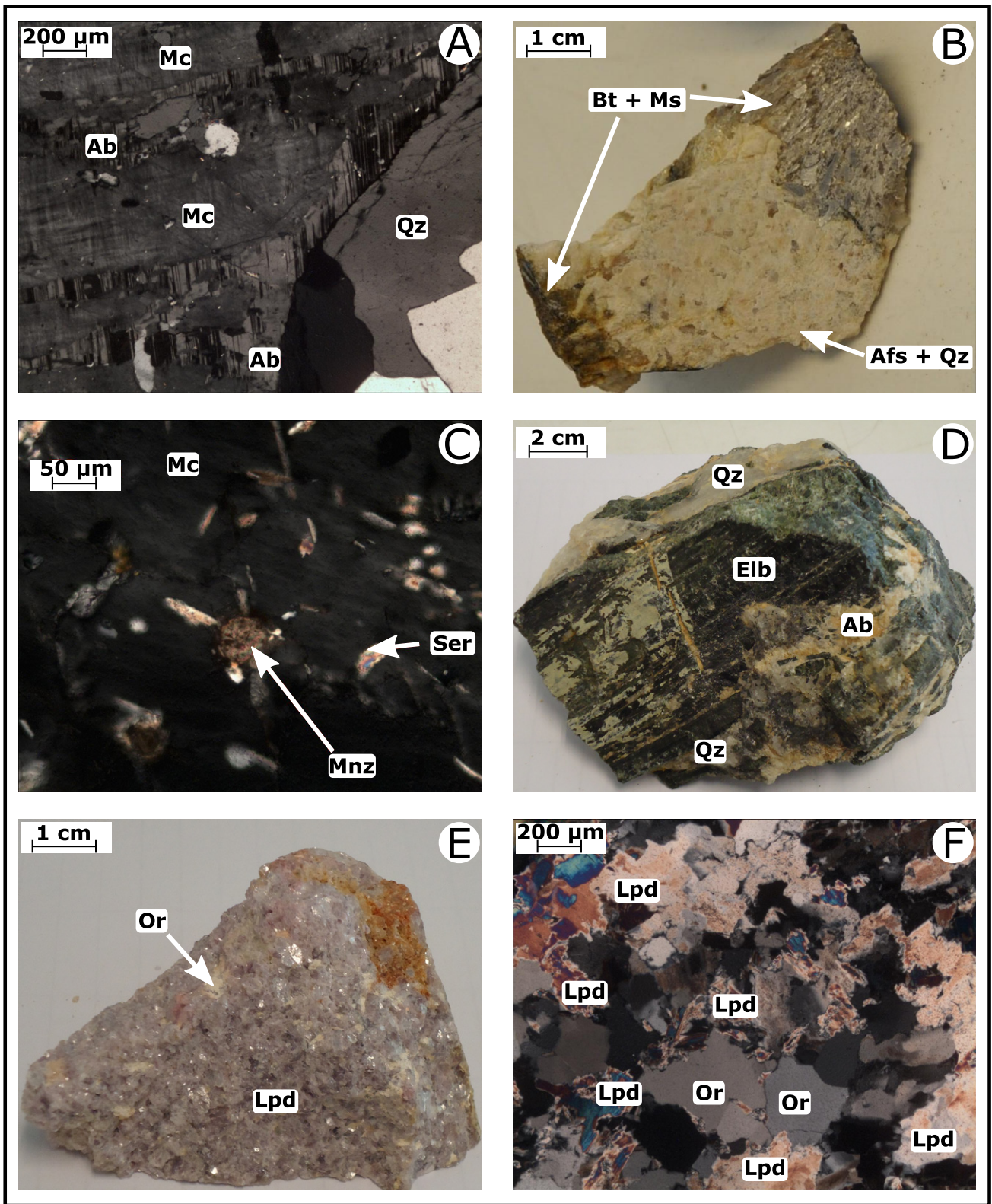


**Plate 1:** (A) Perthite intergrowth textures in a biotite pegmatite with quartz (Qz) of zone 1 with lamellae of microcline (Mc) demonstrating a tartan plaid and primary albite-oligoclase (Ab) polysynthetic twinning (crossed polars). (B) Intergrowths of biotite (Bt) and muscovite (Ms) in a biotite-muscovite-tourmaline pegmatite of zone 3 with K-feldspar (Afs) and quartz (Qz). (C) Monazite (Mnz) accessory included in a weakly sericitised (Ser) microcline (Mc) grain of a biotite-muscovite-tourmaline pegmatite (crossed polars). (D) Quartz core (Qz) with elbaite (Elb) of a zone 6 mineralised pegmatite. The albite (Ab) is secondary in origin and of the cleavelandite habit. (E) Lepidolite (Lpd) can be observed in the Gatumba area as massif, fine-grained, and non-aligned, violet-gray to lavender-coloured aggregates in zone 7 mineralised pegmatites and is associated with traces of orthoclase (Or). (F) Microscopic traces of orthoclase (Or) and quartz are present inside the replacing lepidolite (Lpd) matrix, implying a distinctly secondary origin (crossed polars).